Supplementary Information

Table of contents

Supplementary Information 1

Age at death estimation

Summary: We compare the cortical bone thickness of the *Denisova 11* specimen to a panel of present-day and ancient hominin long bones. Under the conservative assumption that the bone fragment comes from the thickest part of a femur, tibia or humerus, we estimate that the *Denisova 11* individual was at least 13 years old at death.

The Denisova 11 specimen

The *Denisova 11* bone fragment was excavated from square Д-2, in the lower part of Layer 12 of the East Gallery of Denisova Cave in southern Siberia (Russia) in 2012. Given its small size and the lack of diagnostic features, the bone fragment was classified as undiagnostic. The specimen (original sample ID "*DC1227*") was later analyzed by collagen peptide mass fingerprinting, along with 2,314 other undiagnostic remains from the site, resulting in its identification as a hominin bone[3]. CT scanning of the specimen was undertaken by Dr Fiona Brock at Cranfield University using a Nikon XT H 225 micro-scanner with a transmission target. Attempts to keep the dosage as low as possible were made in order to avoid any damage to the sample, so the scan was run at 70 kv and 80 μA (see ref. [3]). Micro-CT scan and 3D print data files are available at: https://doi.org/10.5284/1047219.

Preservation

The specimen is an elongated, about 24.7 mm long, splinter of the cortical part of a large long bone. Based on coloration and texture, the piece preserves the periosteal surface, even though it looks eroded and pitted. It is not completely clear whether the actual endosteal (medullary) surface is preserved, so the cortical thickness of 8.4 mm is a minimum value. The surface, especially periostally, is chemically eroded, possibly due to carnivore digestion.

Identification

When identifying isolated and fragmentary bones, four primary questions are: the taxonomic identification, the anatomical element, and the age and sex of the individual. Gross morphology does not allow us to easily answer any of these questions in this case, but molecular and microstructural approaches allow at least a few tentative conclusions.

The molecular analyses show that the individual was a female archaic hominin, so the remaining questions are the anatomical element the fragment derives from, and the age of the individual. Based on the at least 8.4 mm cortical thickness, the anatomical element is a large long bone, most likely a femur, tibia or humerus because radii, ulnae and fibulae rarely reach such dimensions.

Age at death

Two approaches could in principle be used to estimate the age at death of *Denisova 11*: firstly, the cortical bone thickness of long bones which increases with age[39]; and secondly, changes in bone microstructure that are age-dependent (*e.g.,* [40-42]). Unfortunately, the µCT scans of the specimen[3] lack the resolution needed for an exact assessment of bone microstructure.

Numerous studies show the increasing robusticity of the long bones during ontogeny[43-45], based on measurements of cross-sectional geometry. Not knowing which bone and which portion of the bone we are looking at, we conservatively compare it to the maximum cortical thickness found in long bones. Goldman and colleagues[41] published measurements of cortical thickness at the femoral midshaft. In their toddler (2-3 years), young child (5 years) and older child (9-11 years) categories, the cortical thicknesses are far below that seen in *Denisova 11*, but their 14-16 year-olds reached 8.4 mm posteriorly, a value comparable to *Denisova 11*.

For more extensive comparisons we used Central European Bronze Age children who had been CT scanned[46] and measured the maximum thickness of the cortical wall of their femora, tibiae, humeri, radii and ulnae. The youngest individuals with a maximum cortical thickness similar to that seen in *Denisova 11* were over 13 years of age (Extended Data Figure 1). The maximum thickness was either at the anterior margin of the tibia or near the linea aspera on the femur. However, as far as preservation allows us to tell, *Denisova 11* does not derive from either of these areas, making the age estimate conservative.

One confounding factor is the higher postcranial robusticity of pre-modern humans (*e.g.*, [43,47,48]). On average, Neandertal bones have larger cross sectional areas than modern human bones, even if they fall in the range seen in modern samples[45]. Therefore, we also include in our analysis two juvenile Neandertals from Central Asia. Maximum thicknesses of the femora and humeri in these individuals were similar to modern humans of similar age, supporting that *Denisova 11* was older than these individuals when she died.

Comparative sample and methods

We used Early Bronze Age child skeletons (n=18) from the Anthropology Department, Natural History Museum Vienna. They ranged in age from about 0.5 years to 18 years (for details see Supplementary Table 1.1) based on estimates made by researchers of the Anthropology Department, Natural History Museum Vienna using the methods of Ferembach et al.[49]. The Central Asian Neandertal bones were the "*Okladnikov 7*" & "*Okladnikov 8*" humerus and femur, likely belonging to the same 8-10 year-old individual[46], and the "*Sel'ungur 1*" humerus, deriving from a 10-12 year-old juvenile[50].

The Okladnikov postcrania were scanned by Heiko Temming at the MPI for Evolutionary Anthropology in Leipzig using a BIR ACTIS 225/300 industrial CT, at a resolution of 0.1439 mm (isovoxels). The Sel'ungur humerus was scanned at the Tashkent Kuk-Saroy hospital's GE Lightspeed VCT scanner in 2013 at a resolution of 0.1875 mm, and a slice thickness of 0.625 mm. The modern human right femora, tibiae, humeri, radii and ulnae were scanned with a Philips Brilliance 64 slice CT scanner at the Radiology Department of the Medical University Vienna in 2007. Final resolution depended on the size of the bones, but was between 0.175 and 0.35 mm. Slice thickness and distance was 1 mm.

The maximal diaphyseal cortical thickness was measured in each long bone using *Avizo 8.0*. Going through the diaphysis proximodistally slice by slice, we measured the distance between the periosteal and endosteal surfaces in each slice and used the maximum values found in the bone for comparison.

Supplementary Table 1.1. List of specimens used.

Specimen	Age	Sample
Hainburg 291	7-9	Recent
Hainburg 21074	11-12	Recent
Hainburg 21080	7-9	Recent
Hainburg 21086	14-16	Recent
Hainburg 21088	6-8	Recent
Hainburg 21089	10-12	Recent
Hainburg 21093	14-16	Recent
Hainburg 21105	13-15	Recent
Hainburg 21113	10-11	Recent
Hainburg 21119	15-18	Recent
Hainburg 21122	7-9	Recent
Pottenbrunn 22444	6-8	Recent
Pottenbrunn 22463	4-6	Recent
Pottenbrunn 22465	7-9	Recent
Pottenbrunn 22471	6 months	Recent
Pottenbrunn 22476	2.5	Recent
Pottenbrunn 22501	9 months	Recent
Okladnikov 7 & 8 (humerus and femur only)	8-10 years	Neandertal
Sel'ungur (humerus only)	10-12 years	Neandertal

Supplementary Information 2

Authentication and estimates of contamination by present-day human DNA

Summary: The DNA libraries prepared from the *Denisova 11* specimen contain ancient DNA, as attested by the presence of nucleotide substitutions typical of ancient DNA in the fragments sequenced. The extent of contamination by present-day human DNA in the sequencing data generated from *Denisova 11* was assessed using three different methods. Overall, we estimate that contaminating human DNA fragments constitute at most 1.7% of the data. By comparing these results with previously published data from the same specimen, we show that treating the bone powder with 0.5% sodium hypochlorite solution reduced the proportion of contamination by present-day human DNA.

Authentication using nucleotide substitutions characteristic of ancient DNA

The most common type of chemical damage in ancient DNA is that cytosines (C) near the ends of DNA fragments undergo deamination to uracils, leading to the incorporation of thymine (T) bases by DNA polymerases. Thus, towards their ends, ancient DNA fragments tend to carry C to T substitutions compared to a reference genome. This can be used to authenticate that ancient DNA molecules are present in a DNA library[51-53].

We evaluated the frequencies of nucleotide substitutions compared to the human reference genome (modified version of the human reference hg19/GRCh37 from the 1000 Genomes project (ftp://ftp.1000genomes.ebi.ac.uk/vol1/ftp/technical/reference/phase2_reference_assembly_sequence/)) in the DNA fragments sequenced from *Denisova 11*. Of the fragments starting or ending at alignment positions where the base in the reference genome is a C, 31.4% and 34.4% carried a T at their 5'- and 3'-ends, respectively (Supplementary Table 2.1). These frequencies are higher than for any other type of nucleotide substitutions throughout the fragments (Supplementary Figure 2.1) and higher than expected for present-day DNA (up to 5% in samples dated to ~100 years or younger)[54]. We conclude that the DNA libraries contain at least some DNA fragments of ancient origin.

Additionally, we isolated *in silico* DNA fragments carrying a C to T substitution to the reference genome within their first three or last three bases[55], and computed the frequencies of C to T substitutions on their opposite end. The frequencies of such "conditional" C to T substitutions

can be used as a proxy for the deamination-derived damage expected in the DNA fragments endogenous to the ancient specimen[1]. We find that 32.7% and 35.5% of putatively damaged fragments carry a C to T substitution at their 5'- or 3'-ends, respectively (Supplementary Table 2.1, Supplementary Figure 2.1). The slight increase between the C to T substitution frequencies computed on all fragments and the "conditional" substitutions suggests that while the dataset contains a mixture of deaminated and non-deaminated DNA fragments[1], the latter do not constitute a large proportion of the data. Assuming that the conditional substitutions represent the true C to T substitution frequency in the endogenous fragments and that no deamination signal is present in the contaminants, we estimate that the proportion of contaminating DNA among all aligned fragments is ~3-4%. Given that this measure provides only a rough estimate of contamination with present-day DNA[1], we used three additional methods to evaluate the extent of contaminating human DNA in our dataset.

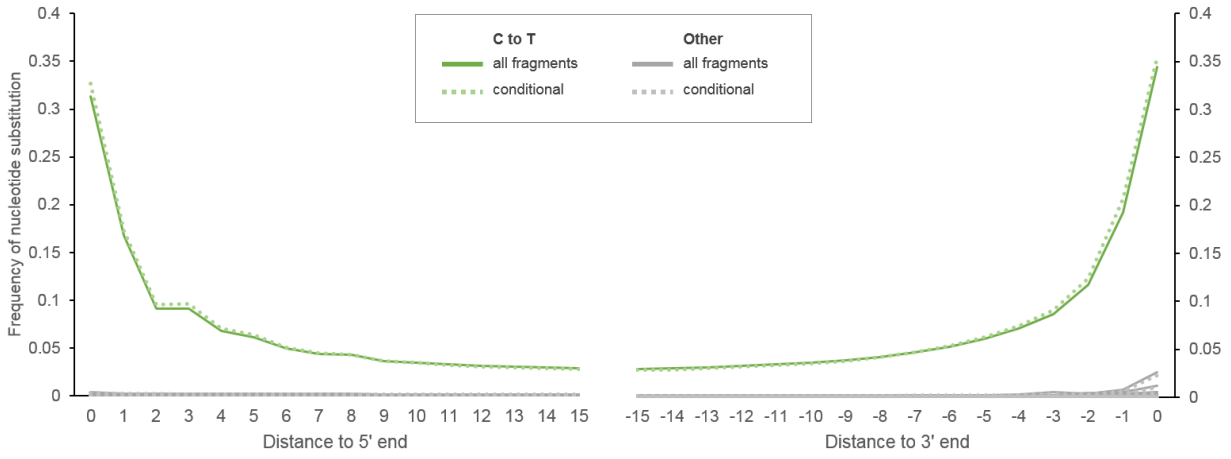

Supplementary Figure 2.1. Frequency of nucleotide substitutions to the human reference genome along the fragments sequenced from *Denisova 11*. Cytosine to thymine (C to T) substitutions are shown in green, all other types of substitutions in grey. The frequencies of "conditional" substitutions are calculated out of fragments presenting a C to T substitution to the reference genome on the opposite end.

Estimate of autosomal contamination using modern human-derived sites

We estimated the extent of contamination by modern human DNA as the proportion of contaminant fragments over the total number of unique mapped fragments passing the filtering scheme detailed in the Methods section (*i.e.*, L≥35, MQ≥25, mappability track Map35_100% from ref. [8]). To determine whether DNA fragments originate from present-day human contamination, we evaluated the base they carry at sites in the genome where previously sequenced archaic individuals differ from modern humans[1,2]. We considered 20,152 informative positions on the autosomes where the three archaic genomes sequenced to high-coverage (*Denisova 3*, the *Altai Neandertal* and *Vindija33.19*)[2,6,8] are all homozygous for the ancestral allele, whereas at least 99% of present-day humans from the 1000 Genomes Phase III (ref. [56]) and the Simons Genome Diversity Project (SGDP)[28] datasets carry the derived allele(s). The ancestral state was defined as an allele shared in a homozygous state by the genomes of a chimpanzee[57] (*panTro4*), a gorilla[58] (*gorGor3*), an orangutan[59] (*ponAbe2*) and a bonobo[60] (*panpan1*). To mitigate the effect of nucleotide substitutions due to deamination, we applied a "strand orientation filter" by considering only strands in reverse orientation when either the ancestral or derived allele is a C; and only strands in forward orientation when one of the informative alleles is a G (ref. [2]). Fragments carrying the human derived allele(s) are considered as contaminants. The estimates of contamination are reported along with binomial 95% confidence intervals calculated using the number of contaminant fragments and the total number of sequenced fragments. As some of the derived variants may have also been present in the archaic populations, we note that these estimates are likely to be over-estimates of the contamination[1]. The present-day human contamination estimate is 1.4% (95% CI: 1.3-1.6%) in the combined dataset when using all DNA fragments; and 1.3% (95% CI: 0.9-1.7%) when retaining only fragments with evidence of deamination, *i.e.*, which carry a T within their first three or last three bases where the reference genome carries a C (Supplementary Table 2.2).

Sexing and Y-chromosome contamination

To determine the sex of *Denisova 11*, we computed the ratio between the average coverage of the X chromosome and the average coverage of the autosomes. This ratio is expected to be 1 in a female and 0.5 in a male. Whether using all fragments in our dataset or restricting to fragments carrying a T within their first three or last three bases where the reference genome is a C, the

coverage of the X chromosome is similar to that of the autosomes (X-to-autosome ratio of 1.1 and 1.0, respectively), indicating that *Denisova 11* was a female.

We estimated the contamination from present-day male DNA by comparing the number of DNA fragments mapping to the Y chromosome to the number expected had the individual been a male. The expectation for a male was calculated by multiplying the number of mapped fragments by the proportion of uniquely alignable positions in the genome that fall on the Y chromosome (within Map35_100% from ref. [8]). We estimate that 1.6% (binomial 95% CI: 1.5-1.7%) of all fragments, and 1.5% (95% CI: 1.3-1.6%) of putatively deaminated fragments, are derived from male DNA (Supplementary Table 2.2).

Mitochondrial DNA contamination

To estimate the contamination by present-day human mitochondrial (mt) DNA, we realigned the reads generated on the first sequencing run performed from each library to the revised Cambridge Reference Sequence (rCRS, NC_012920.1) using BWA[38] with parameters adjusted to ancient DNA[6]. A total of 21,749 unique DNA fragments at least 35 bases long and mapping to the rCRS with a quality of 25 or higher were retained. We then evaluated the fragments overlapping the 72 positions where the previously reconstructed mitochondrial genome of *Denisova 11* (ref. [3]) differs from all mtDNA sequences in a world-wide panel of 311 present-day humans[61]. Fragments matching the present-day human state were considered to originate from contamination. A "strand orientation filter" was applied, and the contamination estimates and their binomial 95% confidence intervals were calculated using the fraction of contaminant fragments among all sequenced fragments mapping to the human mtDNA. Using this approach, we estimate that 0.3% (95% CI: 0.1-0.7%) of mtDNA fragments originate from present-day human contamination in the entire dataset. After retaining only putatively deaminated fragments presenting a C to T substitution to the rCRS at their first three or last three bases, we estimate the present-day human mtDNA contamination to be 0.4% (95% CI: 0.1-1.6%) (Supplementary Table 2.2).

Sodium hypochlorite treatment to reduce contamination

The treatment of bone or tooth powder with 0.5% sodium hypochlorite solution has been shown to reduce contamination by both microbial and present-day human DNA[7,19] without inducing detectable levels of nucleotide substitutions derived from cytosine deamination[19]. We treated five

samples of bone powder from *Denisova 11* with 0.5% sodium hypochlorite solution for 15 minutes[19] and one sample for 30 minutes (see Methods section, Extended Data Table 1), and compared the outcome of these treatments with data from an untreated sample of bone powder of similar mass collected from *Denisova 11* previously[3]. As expected, exposure of the bone powder to sodium hypochlorite reduced the total number of DNA molecules contained in the libraries[19]. The DNA library that was generated following a 30-minute pre-treatment (R9873) was estimated by digital droplet PCR[30] to contain ~3 times fewer DNA molecules than the libraries prepared following a 15-minute pre-treatment (R5507 and R5509) (Extended Data Table 1), and ~50 times fewer molecules than an untreated library (3.96E+09 molecules in library L5502 from [3]).

The percentage of DNA fragments mapping to the human reference genome varied between 1.8% and 13.2% in the libraries prepared after a 15-minute treatment, showing that there is variation among samples in the efficiency of microbial contamination removal. The percentage of mapped fragments was highest (27.9%) after a 30-minute pre-treatment (Extended Data Table 1). However, due to the relatively low content of DNA molecules in the library after this treatment, the overall number of informative fragments (*i.e.*, fragments that pass our filtering scheme) recovered was similar to the shorter treatment.

Contamination by present-day human mtDNA in the previously prepared library without sodium hypochlorite treatment was 7.5% (as estimated using an approach similar to the one described above[3]). In comparison, point estimates of mtDNA contamination were between 0% and 2.2% after sodium hypochlorite treatment for 15 minutes, and 0.1% after 30 minutes (Supplementary Table 2.2).

Supplementary Table 2.1. Frequencies of terminal cytosine (C) to thymine (T) substitutions to the human reference genome. The percentage of DNA fragments presenting a C to T substitution at a terminal alignment position was computed using all fragments sequenced, and after retaining only fragments showing a C to T substitution on their other end ("conditional substitutions"). Results are shown for each library prepared from *Denisova 11* and for the combined dataset. 95% binomial confidence intervals are in parentheses.

	All fragments		**Fragments with C to T on opposite end**	
Indexed library ID	**C to T on 5' end** ***(95% CI)***	**C to T on 3' end** ***(95% CI)***	**C to T on 5' end** ***(95% CI)***	**C to T on 3' end** ***(95% CI)***
R5507	35.9 *(35.8-36.1)*	38.3 *(38.1-38.5)*	36.2 *(35.6-36.8)*	38.6 *(38.0-39.3)*
R5509	39.7 *(39.5-39.9)*	41.6 *(41.4-41.8)*	39.7 *(39.0-40.4)*	41.6 *(40.9-42.3)*
R5780	31.7 *(31.3-32.2)*	35.4 *(34.8-36.1)*	34.2 *(32.1-36.2)*	37.0 *(34.8-39.2)*
R9880	31.5 *(31.4-31.5)*	32.5 *(32.5-32.6)*	32.4 *(32.2-32.6)*	32.9 *(32.7-33.1)*
R9881	31.6 *(31.5-31.6)*	34.2 *(34.2-34.3)*	32.3 *(32.0-32.5)*	34.5 *(34.2-34.7)*
R5782	31.6 *(30.9-32.3)*	32.6 *(31.8-33.5)*	31.7 *(28.7-34.8)*	30.4 *(27.5-33.4)*
R5783	28.1 *(27.6-28.5)*	30.6 *(30.0-31.2)*	30.3 *(28.3-32.3)*	31.5 *(29.5-33.6)*
R9882	27.6 *(27.5-27.6)*	28.6 *(28.5-28.6)*	29.2 *(29.0-29.4)*	29.7 *(29.5-29.9)*
R9883	27.8 *(27.7-27.8)*	31.6 *(31.5-31.6)*	29.4 *(29.2-29.6)*	33.0 *(32.7-33.2)*
R9873	37.9 *(37.8-37.9)*	45.6 *(45.5-45.7)*	37.4 *(37.2-37.6)*	44.9 *(44.7-45.1)*
Combined dataset	**31.4** *(31.3-31.4)*	**34.4** *(34.4-34.4)*	**32.7** *(32.6-32.7)*	**35.5** *(35.4-35.6)*

Supplementary Table 2.2. Estimates of contamination by present-day human DNA. For each method, the percentage of contamination was computed using all fragments, and after retaining fragments showing a C to T substitution to the reference genome within their first three or last three bases. Results are shown for each DNA library and for the combined dataset. 95% binomial confidence intervals are in parentheses.

Indexed library ID	Sodium hypochlorite treatment [minutes]	Autosomal contamination estimate				Mitochondrial DNA contamination estimate	
		Matching present-day human derived alleles *(95% CI)*		Y chromosome contamination *(95% CI)*		Matching present-day human state *(95% CI)*	
		All fragments	Fragments with C to T	All fragments	Fragments with C to T	All fragments	Fragments with C to T
R5507	15	6.8 *(4.5-9.9)*	3.3 *(0.4-11.5)*	3.0 *(2.3-3.7)*	2.2 *(1.1-3.8)*	0.0 *(0.0-23.2)*	0.0 *(0.0-70.8)*
R5509	15	9.7 *(6.3-14.2)*	2.0 *(0.1-10.5)*	5.5 *(4.5-6.8)*	3.6 *(2.0-5.7)*	0.0 *(0.0-28.5)*	0.0 *(0.0-60.2)*
R5780	15	1.9 *(0.4-5.5)*	0.0 *(0.0-45.9)*	1.9 *(0.5-4.9)*	2.3 *(0.1-12.3)*	0.0 *(0.0-6.7)*	0.0 *(0.0-33.6)*
R9880	15	1.2 *(0.9-1.6)*	1.2 *(0.5-2.4)*	1.5 *(1.3-1.7)*	1.4 *(1.1-1.8)*	0.0 *(0.0-1.3)*	0.0 *(0.0-6.1)*
R9881	15	1.0 *(0.7-1.4)*	1.4 *(0.6-2.6)*	1.5 *(1.3-1.7)*	1.4 *(1.0-1.8)*	0.0 *(0.0-1.8)*	0.0 *(0.0-7.3)*
R5782	15	5.6 *(0.1-27.3)*	0.0 *(0.0-97.5)*	2.0 *(0.2-7.1)*	0.0 *(0.0-16.1)*	0.0 *(0.0-11.9)*	0.0 *(0.0-41.0)*
R5783	15	1.5 *(0.0-7.8)*	0.0 *(0.0-41.0)*	2.1 *(0.7-4.7)*	2.3 *(0.1-12.0)*	0.0 *(0.0-5.1)*	0.0 *(0.0-33.6)*
R9882	15	1.3 *(1.0-1.7)*	0.8 *(0.3-1.7)*	1.5 *(1.4-1.7)*	1.4 *(1.0-1.8)*	0.4 *(0.0-2.0)*	0.0 *(0.0-6.2)*
R9883	15	1.2 *(0.9-1.5)*	0.7 *(0.2-1.7)*	1.4 *(1.2-1.5)*	1.5 *(1.1-1.9)*	2.2 *(0.7-5.1)*	3.5 *(0.4-11.9)*
R9873	30	1.6 *(1.2-2.0)*	2.0 *(1.2-3.1)*	1.7 *(1.5-1.9)*	1.4 *(1.1-1.7)*	0.1 *(0.0-0.6)*	0.0 *(0.0-1.8)*
Combined dataset		**1.4** *(1.3-1.6)*	**1.3** *(0.9-1.7)*	**1.6** *(1.5-1.7)*	**1.5** *(1.3-1.6)*	**0.3** *(0.1-0.7)*	**0.4** *(0.1-1.6)*

Supplementary Information 3

The sequencing data originate from a single individual

Summary: The signal of mixed ancestry in the *Denisova 11* genome is consistent across several DNA libraries prepared independently from the specimen, whereas the ratio of microbial to hominin DNA varies substantially among libraries. We use a maximum-likelihood approach to infer the number of mtDNA components in the sequencing data, and find no evidence for the presence of more than one ancient mtDNA genome. We conclude that the signal of mixed ancestry is highly unlikely to be due to an accidental mixture of DNA from two individuals.

The signal of mixed ancestry is consistent across DNA libraries

The genomic data generated from *Denisova 11* derive from experiments carried out on several different occasions (see Methods section). The bone fragment was sampled on three different occasions, on different areas of the specimen, resulting in a total of six samples of bone powder used in the present study. The six DNA extracts were prepared on three occasions, and the ten DNA libraries were generated in three different experiments (Extended Data Table 1). The DNA libraries were sequenced on 17 different sequencing runs.

In order to determine whether the mixed Neandertal and Denisovan ancestry could result from the inadvertent combination of DNA or sequences from multiple sources, we repeated the analysis[1] that revealed that *Denisova 11* carries both Neandertal and Denisovan ancestry, for each DNA library independently. We compared the proportions of DNA fragments from *Denisova 11* that match derived alleles inferred to have arisen on each branch of a tree relating the genomes of a Neandertal (*Altai Neandertal*)[8], a Denisovan (*Denisova 3*) and a present-day African (Mbuti)[6] (see Supplementary Information 4). In the ten DNA libraries, the proportion of fragments matching derived alleles in the Neandertal genome varies between 34.9% and 41.5% and the proportion matching Denisovan derived alleles varies between 37.7% and 43.2% (Supplementary Table 3.1), showing that the signal of mixed ancestry appears in all the DNA libraries. In contrast, we note that the relative proportions of human and microbial DNA differ among the libraries, as indicated by the variation in the percentage of fragments mapping to the human genome (between 1.8% and 27.9%, Extended Data Table 1).

In conclusion, it is highly unlikely that an accidental mixture of DNA from two ancient individuals has affected all libraries resulting in approximately equal proportions of Neandertal and Denisovan DNA while the total proportion of hominin DNA varies more than ten-fold. It is also highly implausible that post-sequencing mixture of data from different sources is responsible for the mixed ancestry observed in all libraries analyzed.

A single ancient mtDNA genome is present in the data

If more than one mtDNA genome was present in the libraries, one would expect sites at which two alternative bases are supported by several DNA fragments. However, at sites where more than one base is observed, only single fragments support a second base, despite the presence of 237 sites with at least four overlapping DNA fragments.

To assess whether more than one individual contributed mtDNA to the data generated, or whether errors are sufficient to explain the observed variability, we applied a maximum-likelihood approach[34]. The method uses the number of fragments supporting each variant at positions where sequenced DNA fragments differ, to estimate the proportion of different mtDNAs. To avoid over-estimating the number of components detected due to sequencing errors, a component is deemed present if its inferred frequency in the data is at least 1% (ref. [34]).

Using DNA fragments presenting a C to T substitution to the rCRS within their first three or last three bases while discarding those shorter than 35bp or with a mapping quality lower than 25 (Supplementary Information 2), the model with two mtDNAs estimates a proportion of less than one in a million for the less frequent mtDNA component. Thus, a model with only one mtDNA fits the data better than a model with either two or three mtDNAs (relative likelihood<0.05; Supplementary Table 3.2).

Supplementary Table 3.1. Matching of derived alleles in ancient hominins and a present-day human. The percentage of fragments matching derived alleles seen in each branch of a tree relating the genomes of a Neandertal (*Altai Neandertal*), a Denisovan (*Denisova 3*) and a present-day individual from Africa (Mbuti) are shown for each *Denisova 11* library and for the combined dataset. 95% binomial confidence intervals are in parentheses.

	Matching of derived alleles *(95% CI)*				
Indexed library ID	**All hominins**	**Shared Neandertal-Denisovan**	**Neandertal**	**Denisovan**	**Present-day human**
R5507	98.9 *(98.8-98.9)*	91.7 *(91.0-92.4)*	37.3 *(36.4-38.2)*	40.4 *(39.5-41.3)*	2.6 *(2.3-2.8)*
R5509	96.9 *(96.8-97.0)*	87.6 *(86.6-88.6)*	34.9 *(33.8-36.0)*	37.7 *(36.6-38.7)*	3.4 *(3.1-3.8)*
R5780	99.7 *(99.6-99.8)*	95.6 *(93.7-97.0)*	39.3 *(36.4-42.3)*	43.2 *(40.3-46.2)*	0.5 *(0.2-1.0)*
R9880	99.7 *(99.7-99.8)*	95.4 *(95.2-95.5)*	38.8 *(38.5-39.1)*	42.4 *(42.1-42.7)*	1.1 *(1.1-1.2)*
R9881	99.7 *(99.7-99.8)*	95.4 *(95.3-95.6)*	38.7 *(38.4-39.0)*	42.6 *(42.3-42.9)*	1.1 *(1.1-1.2)*
R5782	98.9 *(98.6-99.1)*	91.7 *(87.8-94.7)*	36.8 *(32.5-41.2)*	41.7 *(37.6-45.9)*	1.4 *(0.7-2.5)*
R5783	99.7 *(99.6-99.8)*	95.6 *(93.9-96.9)*	41.5 *(38.8-44.2)*	41.3 *(38.7-44.0)*	1.6 *(1.1-2.2)*
R9882	99.7 *(99.7-99.7)*	95.3 *(95.2-95.5)*	38.9 *(38.7-39.2)*	42.3 *(42.0-42.6)*	1.1 *(1.1-1.2)*
R9883	99.7 *(99.7-99.7)*	95.4 *(95.3-95.6)*	38.6 *(38.4-38.9)*	42.6 *(42.4-42.9)*	1.1 *(1.1-1.1)*
R9873	99.8 *(99.8-99.8)*	95.4 *(95.3-95.6)*	38.4 *(38.1-38.7)*	42.2 *(41.9-42.5)*	1.2 *(1.1-1.2)*
Combined dataset	**99.7** *(99.7-99.7)*	**95.2** *(95.2-95.3)*	**38.6** *(38.5-38.7)*	**42.3** *(42.2-42.5)*	**1.2** *(1.2-1.2)*

Supplementary Table 3.2. Log likelihood and parameter estimates of models with one or more mtDNA components in the data generated from *Denisova 11*. When more than one mtDNA components is present, their frequency and divergence from the most common one, and among them if more than two, are estimated, for a total of 1, 3 or 7 estimated parameters (*i.e.*, degrees of freedom) for 1, 2 or 3 components, respectively. "Error" indicates the probability that a DNA fragment overlapping a variable site (*i.e.*, where two alternative bases are observed) carries an error. Note that a probability of error of 0.096 corresponds to a total error rate – not restricted to variable sites – of 0.14%.

Model	Parameter	Value
One mtDNA component	Log likelihood	-22847.4
	Error	0.096
Two mtDNA components	Log likelihood	-22847.2
	Error	0.095
	Frequency 2nd component	$<10^{-6}$
	Divergence 1st to 2nd mtDNA	0.046
Three mtDNA components	Log likelihood	-22847.2

Supplementary Information 4

Denisova 11 has both Neandertal and Denisovan ancestry

Summary: To investigate from which hominin group(s) *Denisova 11* originates, we use the proportions of DNA fragments that match derived alleles seen in a Neandertal, a Denisovan and a present-day human. The DNA fragments from *Denisova 11* match the Neandertal and the Denisovan genomes in approximately equal proportions, suggesting that *Denisova 11* has ancestry from both groups. A 3-population test (*f*3-statistics) supports this; and an estimate of Neandertal ancestry in *Denisova 11* based on *f*4-ratios is close to 50%, as expected for an F1 offspring of a Neandertal and a Denisovan.

Attributing Denisova 11 to a hominin lineage using informative positions

To determine the group of hominins from which *Denisova 11* originates, we used a set of "informative" positions[1], where the allele selected at random from the genomes of a Neandertal (either *Altai Neandertal* or *Vindija 33.19*)[2,8], a Denisovan (*Denisova 3*)[6] and/or a present-day Mbuti individual (HGDP00456)[6] is derived. Only genotype calls at positions passing the minimal filters in ref. [2] (http://cdna.eva.mpg.de/neandertal/Vindija/FilterBed) were considered. The ancestral state was defined as the allele shared by at least three of the following genomes: chimpanzee[57] (*panTro4*), bonobo[60] (*panpan1.1* using an in-house alignment), gorilla[58] (*gorGor3*) and orangutan[59] (*ponAbe2*) (allowing the fourth genome to have either missing information or carry a third allele). A total of 10,008,541 informative positions were defined when using the *Altai Neandertal* genome, and 10,050,963 positions when using the *Vindija 33.19* genome. To prevent cytosine deamination from influencing the results, we disregard DNA fragments that originate from DNA strands carrying an apparent T at an informative position. The percentage of fragments matching the derived state out of the total number of fragments overlapping informative positions for each branch in a tree relating the three genomes, with 95% binomial confidence intervals, are given in Supplementary Table 4.1.

When using the *Altai Neandertal* genome, 38.6% (95% CI: 38.5-38.7%) of fragments from *Denisova 11* carry the Neandertal state, while 42.3% (95% CI: 42.2-42.5%) carry the Denisovan state (Fig. 2a), indicating that *Denisova 11* has ancestry from both Neandertals and Denisovans. These estimates remain stable when using the genome of another Neandertal (*Vindija 33.19*) to

define the Neandertal state; and when using only putatively deaminated DNA fragments from *Denisova 11* (Supplementary Table 4.1).

f3-statistic as a formal test of admixture

To test whether the *Denisova 11* genome is the product of admixture between Neandertals and Denisovans, we computed an *f*3-statistic in the form *f*3(*test genome*; Neandertal, Denisovan). A negative score provides evidence for mixed ancestry in the test genome[62]. As comparison, we also performed this test for the ~2.2-fold coverage genome of a Neandertal individual, "*Goyet Q56-1"*, recently sequenced using methods similar to the ones used here[7]. Two DNA fragments were sampled randomly without replacement at all positions covered by at least two fragments from *Denisova 11* (or from *Goyet Q56-1*, respectively). To prevent cytosine deamination from influencing the results, we disregard DNA fragments that go back to DNA strands that carry an apparent T at an informative position. For the high-coverage genomes (*Denisova 3*, *Altai Neandertal* and *Vindija 33.19)*[2,6,8], two alleles were sampled randomly from the genotype calls. Only bi-allelic transversion polymorphisms on the autosomes, that are variable among the three high-coverage genomes and where the genotype calls pass the recommended filters[2] (http://cdna.eva.mpg.de/neandertal/Vindija/FilterBed) were considered. The *f*3-statistic test was carried out using *ADMIXTOOLS*, with errors computed using the Weighted Block Jackknife with default parameters (*i.e.*, equally sized blocks of 5 million base pairs [5 Mb] across all autosomes)[62]. The *f*3 score for *Denisova 11* is significantly negative, whereas this is not the case for *Goyet Q56-1*, suggesting that errors in the low-coverage genomes used do not drive the negative score seen in *Denisova 11* (Supplementary Table 4.2).

Estimates of Neandertal ancestry in Denisova 11 using f4-ratios

We next estimated the proportion of Neandertal ancestry in the genome of *Denisova 11*, again using *Goyet Q56-1* as a control, by computing *f*4-ratios of the form:

$$\hat{a} = \frac{f4(\text{Neandertal 1}, \text{outgroup: } test\ genome, \text{Denisovan})}{f4(\text{Neandertal 2}, \text{outgroup: Neandertal 1}, \text{Denisovan})}$$

One DNA fragment was sampled randomly from either all fragments sequenced from *Denisova 11* (or *Goyet Q56-1*), or from fragments deriving from DNA strands carrying a T within their first three or last three bases where the reference genome carries a C. Only bases with a quality of at least 30 were retained. Under the assumption that *Denisova 11* is more closely related to *Vindija 33.19* than to the *Altai Neandertal* (Supplementary Information 8), as is the case also for *Goyet Q56-1* (ref. [7]), we used the genome of the *Altai Neandertal* as Neandertal 1, of *Vindija 33.*19 as Neandertal 2, and of *Denisova 3* as the Denisovan. One putatively deaminated fragment was sampled at random from these high-coverage genomes[2,6,8], and the outgroup was either the genomes of three Mbuti individuals from the SGDP panel[28] or the genome of a chimpanzee[57] (*panTro2*). We used *heffalump*[7] to identify the variable sites and to format the input files for *ADMIXTOOLS*[62], which was used to compute the *f*4-ratios. Only bi-allelic autosomal transversion polymorphisms among the three high-coverage genomes and within tracks of high-quality genotype calls[2] (http://cdna.eva.mpg.de/neandertal/Vindija/FilterBed) were considered. Standard errors were calculated by Weighted Block Jackknife in blocks of 5 Mb.

Given that other analyses of the genome of *Denisova 11* show that this individual is the direct offspring of a Neandertal and a Denisovan (Supplementary Information 5 and 6), we expected the inferred percentage of Neandertal ancestry to be 50%, or nearly so (Supplementary Information 7). Yet in all schemes of the *f*4-ratio we tested, the inferred percentage is slightly lower. Similarly, the proportion of inferred Neandertal ancestry in the genome of *Goyet Q56-1* tends to be lower than the expected 100% (Supplementary Table 4.3). As it was previously cautioned that errors may bias the *f*4-ratios[62], we used simulations in order to gauge to which extent errors in DNA sequences may affect our results.

We simulated the Neandertal and Denisovan parents of an F1 offspring, following the demography inferred from high-coverage archaic genomes[2], as described in Supplementary Information 6. As predicted, errors in the DNA fragments of *Denisova 11* decrease the estimated proportion of Neandertal ancestry below 50% due to the attraction of *Denisova 11* to the outgroup (Supplementary Table 4.4). Note that in our simulations, the Denisovan parent of *Denisova 11* separates slightly later (by ~10,000 years) from the ancestral population of *Denisova 3* than the Neandertal parent from the ancestral population of *Vindija 33.19* (Supplementary Information 8). Despite this, in the absence of errors, the expected *f*4-ratio is 50%. This indicates that a slightly higher genetic similarity between *Denisova 3* and the Denisovan component of *Denisova 11* than

between *Vindija 33.19* and the Neandertal component would not be sufficient to lower the *f*4-ratio to the extent observed. We also tested whether other demographic factors, such as introgression of Neandertal alleles into Denisovans, may lower the *f*4-ratio, by sampling simulated Neandertal alleles from the same Neandertal parental population of the F1 offspring rather than Denisovan alleles, in varying proportions. However, only a proportion of admixture of at least 5%, *i.e.*, higher than the 0.5% previously estimated[2,8], can reduce the *f*4-ratio below 48%, leaving errors as the most likely explanation for the low observed percentage of Neandertal ancestry in *Denisova 11*.

Supplementary Table 4.1. Attributing *Denisova 11* to a hominin group. The percentage of DNA fragments matching derived alleles in the genomes of a Neandertal (*Altai Neandertal* or *Vindija 33.19*), a Denisovan (*Denisova 3*) and a present-day individual from Africa (Mbuti) are shown, with 95% binomial confidence intervals. Results are shown using all fragments sequenced from *Denisova 11*, and using fragments originating from DNA strands carrying a T within their first three or last three bases where the reference genome carries a C. The number of DNA fragments retained in each analysis is reported.

DNA fragments from *Denisova 11*	Neandertal genome used	Number of fragments at informative sites	Matching of derived alleles *(95% CI)*				
			All hominins	Shared Neandertal-Denisovan	Neandertal	Denisovan	Present-day human
All fragments	*Altai Neandertal*	10,323,808	99.7 *(99.7-99.7)*	95.2 *(95.2-95.3)*	38.6 *(38.5-38.7)*	42.3 *(42.2-42.5)*	1.2 *(1.2-1.2)*
	Vindija 33.19	10,367,378	99.7 *(99.7-99.7)*	96.1 *(96.0-96.2)*	38.9 *(38.8-39.0)*	42.0 *(41.9-42.2)*	1.0 *(1.0-1.0)*
Fragments with C to T	*Altai Neandertal*	2,008,059	99.7 *(99.7-99.7)*	95.3 *(95.2-95.5)*	37.8 *(37.5-38.0)*	41.3 *(41.0-41.6)*	1.1 *(1.1-1.2)*
	Vindija 33.19	2,016,895	99.7 *(99.7-99.7)*	96.2 *(96.0-96.3)*	37.9 *(37.6-38.1)*	41.0 *(40.8-41.3)*	0.9 *(0.9-1.0)*

Supplementary Table 4.2. Testing for admixture between Neandertals and Denisovans. The test was carried out in the form *f*3(*test genome*; Neandertal, Denisovan), using the genome of either *Denisova 11* or *Goyet Q56-1* as the test genome; the genome of either the *Altai Neandertal* or *Vindija 33.19* to represent the Neandertal source; and *Denisova 3* as the Denisovan. The number of informative SNPs in each test is shown.

Test genome	Neandertal source	Denisovan source	n	*f*3	Standard error	Z-score
Denisova 11	*Altai Neandertal*	*Denisova 3*	2,658	-0.356	0.00253	-140.722
	Vindija 33.19	*Denisova 3*	3,449	-0.396	0.00202	-195.845
Goyet Q56-1	*Altai Neandertal*	*Denisova 3*	1,439	1.559	0.04305	36.206
	Vindija 33.19	*Denisova 3*	3,721	0.361	0.01757	20.547

Supplementary Table 4.3. Estimating Neandertal ancestry in *Denisova 11*, and in *Goyet Q56-1* as control. The proportion of Neandertal ancestry was computed using *f*4-ratios in the form *f*4(Neandertal 1, outgroup:test genome, Denisovan)/*f*4(Neandertal 2, outgroup:Neandertal 1, Denisovan). We used the genomes of the *Altai Neandertal* as Neandertal 1, *Vindija 33.19* as Neandertal 2, and *Denisova 3* as the Denisovan. As outgroup, we used either the genomes of three Mbuti individuals or the genome of a chimpanzee. Results are shown when using all fragments from *Denisova 11* or *Goyet Q56-1*, and after retaining only fragments with an apparent C to T substitution to the reference genome within their first three or last three bases. Results are based on n=9,873,264 SNPs, errors are calculated by weighted block jackknife in blocks of 5 Mb (n=556 blocks).

			***f*4-ratio**		
Test genome	**Outgroup**	**DNA fragments from test genome**	**Neandertal ancestry (α)**	**Standard error**	**Z-score**
Denisova 11	Mbuti	All fragments	0.488	0.002	215.98
		With C to T	0.482	0.003	154.52
	Chimpanzee	All fragments	0.475	0.003	189.846
		With C to T	0.473	0.003	140.401
Goyet Q56-1	Mbuti	All fragments	0.984	0.002	420.271
		With C to T	0.996	0.003	319.733
	Chimpanzee	All fragments	0.987	0.002	472.980
		With C to T	0.995	0.003	341.951

Supplementary Table 4.4. Estimating Neandertal ancestry in the simulated genome of a Denisovan-Neandertal F1 offspring. The proportion of Neandertal ancestry was computed using *f*4-ratios in the form *f*4(Neandertal 1, outgroup:test genome, Denisovan)/*f*4(Neandertal 2, outgroup:Neandertal 1, Denisovan), where the outgroup is a simulated genome separated from the human lineage 13 million years ago[22,29], comparable to the human-chimpanzee split time. The per-base error probability is reported in "Error (%)", and the fraction of Neandertal (N) alleles introgressed in the Denisovan (D) genome is simulated by artificially sampling Neandertal alleles from the population ancestral to *Vindija 33.*19 with probability reported in the field "Admixture".

Neandertal 1	**Neandertal 2**	**Admixture**	**Error (%)**	**Neandertal ancestry (α)**
Altai Neandertal	*Vindija 33.19*	0	0	0.500
		0	0.1	0.478
		0	0.2	0.458
		N to D 0.5%	0	0.496
		N to D 5%	0	0.473

Supplementary Information 5

Heterozygosity estimates

Summary: We use the ancient DNA genotyping software *snpAD* to estimate the frequency of all possible heterozygous genotypes in the low-coverage *Denisova 11* genome and in a subset of the data of the high-coverage *Vindija 33.19* Neandertal genome which is similar in coverage and ancient DNA damage patterns to *Denisova 11*. We find that the transversional heterozygosity in *Denisova 11* is 3- to 6-fold higher than in *Vindija 33.19* and similar to the average nucleotide differences between the high-coverage Denisovan and either of the two high-coverage Neandertal genomes.

In genomic regions where both chromosomes of *Denisova 11* seem to be derived from Neandertals (Supplementary Information 7), the estimated heterozygosity is substantially lower than the genome-wide estimates but higher than in the same regions in the genomes of *Vindija 33.19* or the *Altai Neandertal*, raising the possibility that the Neandertals that contributed to *Denisova 11* were from different populations.

Data and initial processing

We use approximately 2-fold coverage data from library A9369 of *Vindija 33.19* (ref. [2]). This library was prepared with a single-stranded DNA library preparation protocol[19,20] and not treated to remove uracils that give rise to apparent C to T substitutions[51,63], matching the properties of the *Denisova 11* data (see Methods section). Following previous approaches[2,7], all data were filtered for fragments of at least 35bp length and a minimum mapping quality of 25. Input files for *snpAD*[2] were generated and filtered for mappable positions (Map35_100% in SI5b of [8]).

Estimating error profiles

An error model for miscalled bases in the individual DNA fragments sequenced is required by the genotyping software to derive estimates of the frequency of all possible genotypes by maximum likelihood. The error models for previously genotyped ancient genomes were derived by comparison to a preliminary consensus or by comparison to a closely related genome sequence[2].

Since the *Denisova 11* data shows high similarity to both Neandertal and Denisovan genomes (Supplementary Information 4), we partition the sequenced DNA fragments into those

that carry the *Vindija 33.19* Neandertal allele and those that carry the *Denisova 3* (ref. [6]) Denisovan allele where the two high-coverage genomes differ and are homozygous. We then derive an error model by comparing the resulting 1.4 million Denisovan-matching and 1.3 million Neandertal-matching DNA fragments and counting substitutions.

We repeat this process for the subset of the *Vindija 33.19* Neandertal data and estimate an error model from 2.5 million Neandertal-matching fragments and 40,000 Denisovan-matching fragments. The resulting error model matches the error model derived from the high-coverage genome sequence well (Pearson correlation r>0.999; Supplementary Figure 5.1).

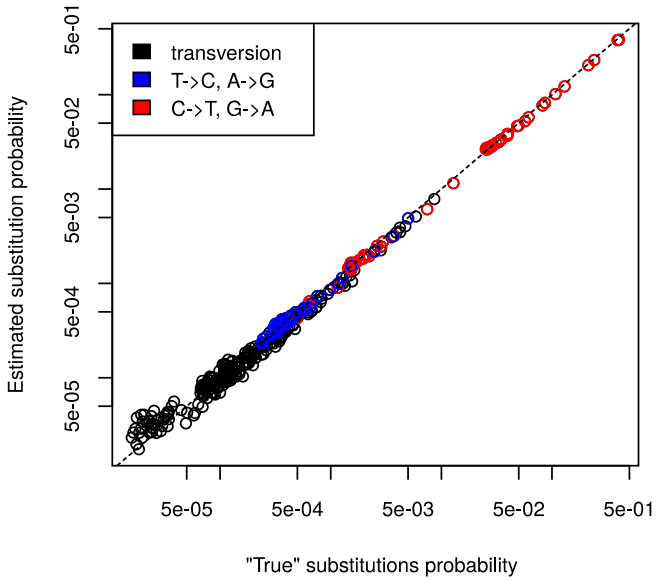

Supplementary Figure 5.1. "**True" versus estimated error models.** Estimated position-dependent substitution probabilities are calculated from sequenced DNA fragments assigned to the Neandertal or the Denisovan genome based on informative sites. "True" substitution probabilities are calculated by comparing sequenced DNA fragments to the consensus of the high-coverage *Vindija 33.19* genome. Dashed line indicates equality.

Estimating heterozygosity in a subset of the Vindija 33.19 data

To test whether heterozygosity can be estimated from low-coverage genomes, we first applied *snpAD* to each autosome using the 2-fold coverage *Vindija 33.19* data and the error model described above. Compared to the estimates from the high-coverage data, the probabilities of CT and AG heterozygotes are higher (Supplementary Figure 5.2); the presence of C to T and G to A substitutions typical of ancient DNA likely inflates these probabilities. However, estimates of the frequency of transversion heterozygotes are close to the estimates from the full data for all chromosomes (Supplementary Figure 5.2), suggesting that the rate of transversion heterozygotes can be reliably estimated from low-coverage genomes.

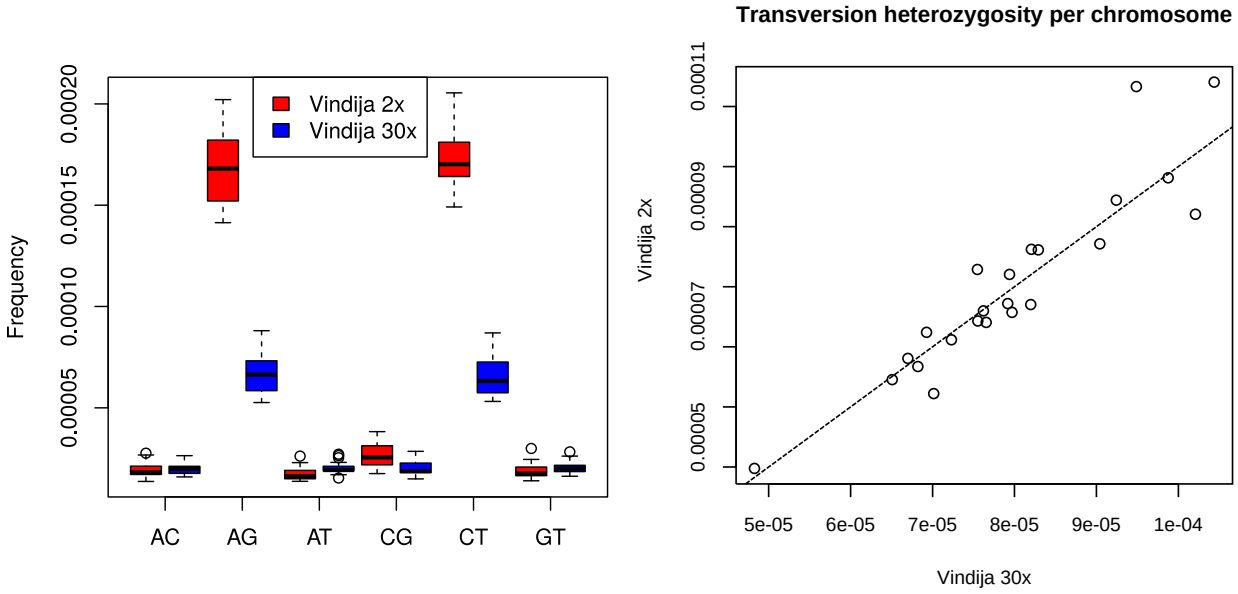

Supplementary Figure 5.2. Heterozygosity estimates for the subsample of the *Vindija 33.19* genome. **Left:** Estimated frequency of different heterozygous states for the *Vindija 33.19* 2-fold coverage subset and the full 30-fold coverage data. Boxes indicate the range over autosomes (labelling according to defaults in the R boxplot function: top and bottom of box indicate 25th and 75th percentile [interquartile range, IQR]; bold line in the box indicates median; error bars indicate 1.5 x IQR or maximum value, whichever is smaller). **Right:** Frequency of transversion heterozygotes (sum over AC, AT, CG and GT frequency) per chromosome for the full *Vindija 33.19* data and the 2-fold subset. Dashed line indicates equality.

Estimating heterozygosity in Denisova 11

We estimated the transversion heterozygosity for *Denisova 11* (Supplementary Figure 5.3). In a per-chromosome comparison to *Vindija 33.19*, the transversion heterozygosity is a factor of 3.2-5.8 higher in the *Denisova 11* individual.

To test whether the high heterozygosity is in the range of the heterozygosity expected for an F1 offspring of a Neandertal and a Denisovan, we calculated the frequency of transition and transversion differences between the high-coverage *Vindija 33.19* and *Denisova 3* genomes. We find that the frequency of different heterozygous sites is generally similar to that expected for an individual that carried one set of chromosomes from *Vindija 33.19* and one from *Denisova 3* (Supplementary Figure 5.3). However, the estimated transition heterozygosity tends to be slightly higher while the transversion heterozygosity tends to be slightly lower for *Denisova 11* compared to this expectation (Supplementary Figure 5.3).

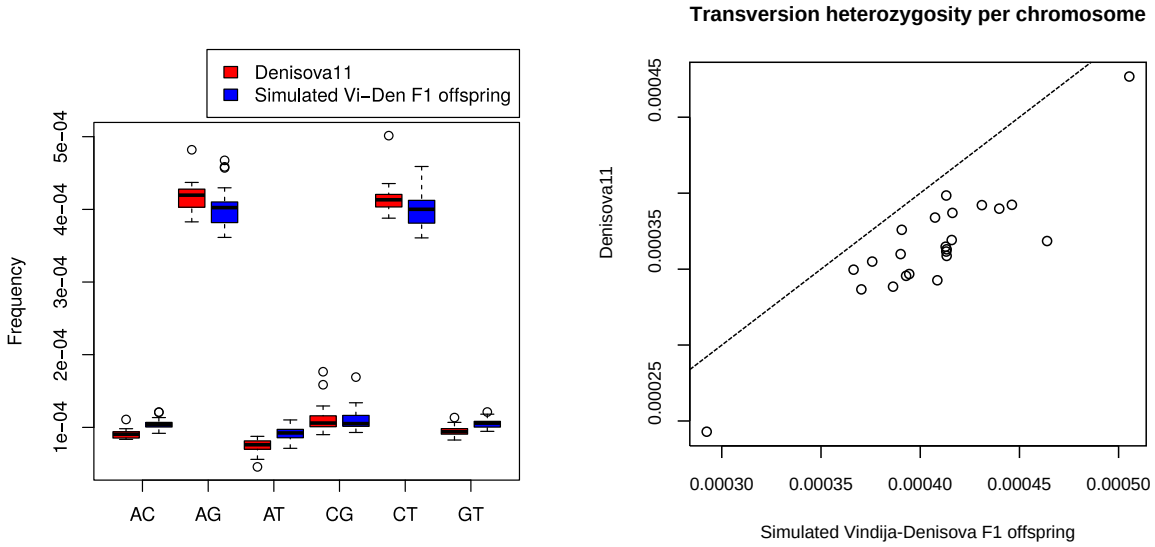

Supplementary Figure 5.3. Heterozygosity estimates for *Denisova 11*. Left: Estimated frequency of different heterozygous states for *Denisova 11* compared to the expectation for a hypothetical F1 offspring of *Vindija 33.19* and *Denisova 3*. Boxes indicate the range over autosomes (labelling as in Supplementary Figure 5.2). **Right**: Frequency of transversion heterozygotes (sum over AC, AT, CG and GT frequency) per chromosome for *Denisova 11* and the hypothetical F1. Dashed line indicates equality. The two chromosomes with the lowest and highest heterozygosity, respectively, are X and 16.

Heterozygosity in Neandertal-ancestry regions in Denisova 11

Other analyses indicate that some regions in the *Denisova 11* genome harbor ancestry from Neandertals on both chromosomes (Supplementary Information 7). Here, we estimate the heterozygosity in these regions. For this, we extract data for the five longest regions, spanning a total of 4.2 Mb on chromosomes 3, 6, 9 and 14, and run *snpAD* with the genome-wide error model on the combined data of all five regions. A comparison of the heterozygosity estimates for these regions in the 2-fold *Vindija 33.19* data to the genotypes of the high-coverage *Vindija 33.19* genome shows that the estimated frequencies are only approximate (Supplementary Table 5.1). However, it is interesting to note that all four transversion polymorphisms are more frequent in *Denisova 11* than in *Vindija 33.19* or the *Altai Neandertal*[8], and more similar to the frequency of transversion differences between the two high-coverage Neandertal genomes (Supplementary Table 5.2).

Supplementary Table 5.1. Estimated frequency of polymorphisms in a 2-fold subset and the full 30-fold *Vindija 33.19* genome in regions that have only Neandertal ancestry in *Denisova 11*.

Genotype	*Vindija* 2x	*Vindija* 30x
AC	2.20E-05	1.46E-05
AG	2.10E-04	5.71E-05
AT	1.36E-05	1.99E-05
CG	2.54E-05	1.60E-05
CT	1.58E-04	5.12E-05
GT	2.03E-05	1.57E-05

Supplementary Table 5.2. Frequency of polymorphisms within *Denisova 11, Vindija 33.19* and the *Altai Neandertal,* and between *Vindija 33.19* and the *Altai Neandertal*.

Genotype	*Denisova 11*	*Vindija 33.19*	*Altai Neandertal*	*Vindija-Altai*
AC	3.81E-05	1.46E-05	1.53E-05	3.07E-05
AG	1.41E-04	5.71E-05	4.88E-05	1.10E-04
AT	2.12E-05	1.99E-05	2.13E-05	3.62E-05
CG	3.93E-05	1.60E-05	1.43E-05	3.87E-05
CT	1.53E-04	5.12E-05	4.77E-05	1.12E-04
GT	2.84E-05	1.57E-05	1.60E-05	3.90E-05

Supplementary Information 6

Proportions of alleles matching Neandertal or Denisovan genomes

Summary: We show that the proportions of DNA fragments matching Neandertal or Denisovan alleles match those expected for an F1 offspring of Neandertal and Denisovan parents originating from populations with a demographic history similar to those of genomes determined to date.

Proportions of alleles matching Denisovan or Neandertal genomes

At all sites in which two parental chromosomes N (for Neandertal) and D (for Denisovan) differ, the F1 offspring will be heterozygous ND (*i.e.*, 100% ND). For an F2 offspring, *i.e.*, the offspring of two F1 individuals, 50% of the sites will be ND, 25% NN and 25% DD. These proportions coincide with those of a population at Hardy-Weinberg equilibrium where 50% of the ancestry is of Neandertal and 50% of Denisovan origin.

However, since the *Denisova 11* genome is sequenced to low coverage, we are only able to examine the state of two DNA fragments that overlap heterozygous sites. In an F1 individual, these two fragments are expected to carry the NN state in 25% of cases, the heterozygous state ND in 50% of cases, and the DD state in 25%. When two fragments are sampled from the genome of an F2 individual, 37.5%, 25% and 37.5% will be NN, ND and DD, respectively.

In Fig. 2c we analyze positions where the *Altai Neandertal* genome[8] is homozygous (state NN) and differs from the *Denisova 3* Denisovan genome[6] (state DD) by a transversion. The proportions of NN, ND and DD fragments from *Denisova 11* are 27.3%, 43.5% and 29.2%, respectively. When the *Vindija 33.19* Neandertal genome[2] is used instead, these proportions are 26.9%, 43.1% and 30.0%, respectively. Similar proportions are observed when randomly sampling alleles from *Denisova 3* and *Vindija 33.19* (29.0%, 38.6% and 32.3%, respectively). Note that the *Denisova 3* and the two Neandertal genomes are obviously not identical to the parental genomes of *Denisova 11*. Thus, the expectations depend on the genetic similarity of the parents of *Denisova 11* to the genomes that are used for this comparison, which in turn depends on different factors, most importantly the population sizes and substructure of the parental populations and the times of their separations. The lower the genetic similarity, the lower is the expected proportion of ND.

To test if the observed proportions of NN, ND and DD sites in *Denisova 11* are compatible with those expected for a direct offspring (F1) of a Neandertal and a Denisovan, we compared them to those expected given previously estimated relative ages and population sizes of Neandertals and Denisovans[2,6]. We used coalescent simulations, including demographies from PSMC and age estimates from "branch-shortening" for *Denisova 3* and *Vindija 33.19* (refs.[2,6]), and split-time estimates between the high-coverage genomes[2,6,8] and between the parents of *Denisova 11* and the Denisovan and Neandertal lineages (Supplementary Information 8). We assume that *Denisova 11* lived 90,000 years ago (90 kya). We simulated 1 Gb of sites with the software *scrm*[64] using the command line in Supplementary Figure 6.1.

In Extended Data Figure 2a, we show the proportions of NN, ND and DD states at positions where a random allele in *Denisova 3* differs from a random allele in *Vindija 33.19* for an F1 and an F2 offspring of simulated Neandertal (NF0) and Denisovan (DF0) parents, and for *Denisova 11*. For the simulated genomes, we also show the expected proportions of sites in the genomes (Extended Data Figure 2b, "genotypes"). The expectation for an F1 offspring matches the observed proportions of *Denisova 11* better than the F2 offspring scenario (p-value < 10^{-16}, likelihood ratio test with the proportion of genotypes following a multinomial expectation), and also better than the ideal F1 scenario when population relationships are ignored (*i.e.*, 25% NN and DD, 50% ND; p-value < 10^{-16}). We note that the simulations show DD sites to be more frequent (31.4%) than NN sites (29.5%). This could be due to an excess of Denisovan ancestry in the *Denisova 11* genome. However, simulations show that this can also be explained by the higher genetic similarity of *Denisova 3* to the Denisovan parent of *Denisova 11* than of *Vindija 33.19* to her Neandertal parent, a situation suggested by other analyses (Supplementary Information 8).

```
~/bin/scrm-1.7.2/scrm 19 1000 -t 58 -r 52 1000000 -I 5 0 0 0 0 1 -l 100r \
    -transpose-segsites \
    -SC abs \
    -eI .4741379310 2 0 0 0 0 \
    -eI .6034482758 0 0 2 0 0 \
    -eI .9913793103 0 2 0 0 0\
    -eI 0.7758621 0 4 4 4 0 \
    -ej 1.185345 2 1 -en 1.1637931034 1 2.2267 \
    -ej 3.575 3 1 -en 3.575 1 4.8282 \
    -ej 0.8189655 4 1 -en 0.8189655 1 2.4021 \
    -ej 86.2069 5 1 \
    -n 1 0.8507 -n 2 0.3711 -n 3 1.8482 -n 4 0.8507 -n 5 20 \
    -en 0.4741 1 0.8507 -en 0.5112 1 0.3825 -en 0.5357 1 0.9686 -en 0.5654 1 1.4442 -en
0.6012 1 1.8218 -en 0.6446 1 2.1500 -en 0.6970 1 2.3546 -en 0.7604 1 2.4021 -en 0.8370 1
2.3073 -en 0.9297 1 2.2340 -en 1.0417 1 2.2267 -en 1.1772 1 2.1731 -en 1.3409 1 2.0735 -en
1.5389 1 2.0461 -en 1.7784 1 2.1512 -en 2.0678 1 2.3984 -en 2.4179 1 2.7952 -en 2.8410 1
3.4915 -en 3.3527 1 4.8282 -en 3.9714 1 7.1128 -en 4.7194 1 10.0716 -en 5.6239 1 12.6619 -
en 6.7174 1 14.2335 -en 8.0396 1 15.0026 -en 9.6383 1 14.9844 -en 11.5713 1 13.7417 -en
13.9084 1 10.2578 -en 20.1508 1 38.1779 \
    -en 0.9914 2 0.3711 -en 1.0284 2 0.5107 -en 1.0529 2 0.7184 -en 1.0827 2 1.0501 -en
1.1188 2 1.3948 -en 1.1626 2 1.8616 \
    -en 0.6034 3 1.8482 -en 0.6449 3 1.2351 -en 0.6723 3 2.3349 -en 0.7055 3 2.8369 -en
0.7456 3 2.2964 -en 0.7941 3 1.5985 -en 0.8528 3 1.3490 -en 0.9237 3 1.4688 -en 1.0095 3
1.7861 -en 1.1133 3 2.1030 -en 1.2388 3 2.3594 -en 1.3905 3 2.6704 -en 1.5741 3 3.0107 -en
1.7960 3 3.2033 -en 2.0645 3 3.1756 -en 2.3891 3 3.0332 -en 2.7817 3 2.9611 -en 3.2565 3
3.1899  \
    -en 0.4741 4 0.8507 -en 0.5112 4 0.3825 -en 0.5357 4 0.9686 -en 0.5654 4 1.4442 -en
0.6012 4 1.8218 -en 0.6446 4 2.1500 -en 0.6970 4 2.3546 -en 0.7604 4 2.4021 -en 0.8370 4
2.3073 -en 0.9297 4 2.2340 -en 1.0417 4 2.2267 -en 1.1772 4 2.1731 -en 1.3409 4 2.0735 -en
1.5389 4 2.0461 -en 1.7784 4 2.1512 -en 2.0678 4 2.3984 -en 2.4179 4 2.7952 -en 2.8410 4
3.4915 -en 3.3527 4 4.8282 -en 3.9714 4 7.1128 -en 4.7194 4 10.0716 -en 5.6239 4 12.6619 -
en 6.7174 4 14.2335 -en 8.0396 4 15.0026 -en 9.6383 4 14.9844 -en 11.5713 4 13.7417 -en
13.9084 4 10.2578 -en 20.1508 4 38.1779
```

Supplementary Figure 6.1. ***scrm*** **command line used to simulate the demography of** ***Vindija 33.19*** **(population 1), the** ***Altai Neandertal*** **(population 2),** ***Denisova 3*** **(population 3), a Neandertal lineage separating from** ***Vindija 33.19*** **100 kya representing the Neandertal mother of** ***Denisova 11*** **living 90 kya (population 4), and chimpanzees (population 5).** Population size changes, split times and age of the individuals were estimated in ref. [2].

The F1 status of Denisova 11 is supported under different demographic scenarios

To test how stable our results are, we varied the simulated split time between Neandertals and Denisovans (Supplementary Figure 6.2a,b), the split of the Neandertal parent of *Denisova 11* from *Vindija 33.19* (Supplementary Figure 6.2c) and that of the Denisovan parent from *Denisova 3* (Supplementary Figure 6.2d). Within the ranges tested, these parameters affect the proportions of NN, ND and DD sites to extents that are still compatible with *Denisova 11* being an F1 (a multinomial likelihood ratio test comparing the expected proportion of genotypes under an F1 or F2 model always has a p-value $<10^{-6}$, under all combinations of parameters), suggesting that this conclusion is robust.

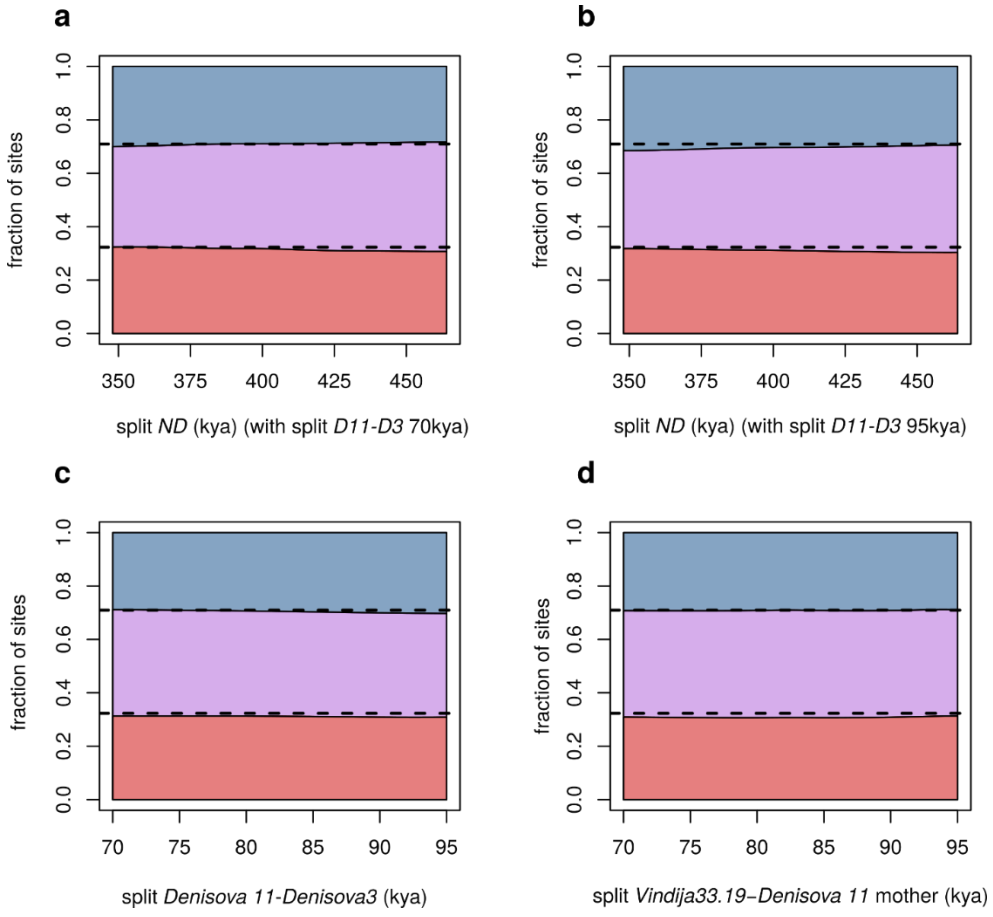

Supplementary Figure 6.2. Expected proportions of NN (blue), ND (purple) or DD (red) sites for 50 sets of *scrm* simulations across each of the varied parameters: the split time between Neandertal and Denisovans when the split of *Denisova 11* from *Denisova 3* is fixed to either 70 kya (**a**) or 95 kya (**b**), the split of the Denisovan father of *Denisova 11* from *Denisova 3* (**c**) and the split time between *Vindija 33.19* and the Neandertal component of *Denisova 11* (**d**). Unless mentioned otherwise, all parameters are fixed to the estimated split times calculated with the F(A|B) method reported in Supplementary Information 8. Dashed lines indicate the observed proportions of NN, ND and DD sites in *Denisova 11*.

Supplementary Information 7

Identifying Neandertal ancestry in the Denisovan father

Summary: Genome-wide signatures show that the *Denisova 11* individual has a Neandertal and a Denisovan parent (Supplementary Information 4-6). Here, we scan the *Denisova 11* genome for regions that deviate from the expected pattern, *i.e.*, we search for regions that show homozygous Neandertal or homozygous Denisovan ancestry. We identify at least five ~1 Mb long regions homozygous for Neandertal ancestry, consistent with the Denisovan father's genome harboring Neandertal ancestry from admixture with Neandertals. Simulations suggest that this admixture occurred between 300 and 600 generations before *Denisova 11* lived.

Scanning the genome for regions homozygous for Neandertal or Denisovan ancestry

For all analyses, we consider only those sites where randomly sampled alleles from the inferred genotypes of the high-coverage *Denisova 3* (ref. [6]) and *Vindija 33.19* (ref. [2]) genomes differ. From *Denisova 11*, we randomly sample, without replacement, two DNA fragments at all such sites that are covered by at least two fragments. Sites where one or both fragments match neither the Neandertal nor the Denisovan state are excluded. For further analysis, we categorize sites into three classes:

- ND: one randomly sampled fragment from *Denisova 11* matched the Neandertal state, the other matched the Denisovan state;
- DD: both fragments matched the Denisovan state;
- NN: both fragments matched the Neandertal state.

We note that since we randomly sample two DNA fragments from *Denisova 11*, at true heterozygous sites we expect 25% of sites to have state NN and 25% of sites state DD.

Qualitatively, individual chromosomes follow a similar two-allele patterns as the genome-wide distribution (Supplementary Figure 7.1). This rules out a situation where a substantial portion of a single chromosome significantly deviates from the genome-wide average, as was the case for *Oase 1*, an ancient modern human with a high proportion of Neandertal ancestry[23].

We next consider 1 Mb windows (with a 100 kb step) throughout the genome, and look for deviations of Neandertal and Denisovan allele counts with respect to the genome-wide average and with respect to simulations. We detect outlier windows using three approaches:

- First, we use a chi-square test of goodness-of-fit to identify windows with Neandertal and Denisovan allele counts that deviate from the genome-wide proportions. The most dramatic outliers are significantly enriched for Neandertal ancestry (Extended Data Figure 3), whereas few windows with significant Denisovan bias are identified. We used a cut-off of chi-square p-value < 10^{-8} to select outlier windows.
- Second, we simulated 10,000 regions of 1 Mb of an F1 offspring of a Denisovan and a Neandertal (Supplementary Information 6), and for each simulated region record the proportion of informative sites which match the Neandertal state (%N). For these simulations, we set a uniform recombination rate such that the standard deviation of %N in simulated windows matched the standard deviation of the observed windows, controlling for the number of informative sites per window (Supplementary Figure 7.2a,b). This yields a recombination rate for the simulations of 0.3315 cM/Mb, smaller than the average genome-wide recombination rate in modern humans (~1.2 cM/Mb; [65]). The low rate is likely due to recombination rate heterogeneity (*i.e.*, hotspots), which would also reduce the number of independent observations per window by linking many sites. Similar to the previous test, there is an excess of Neandertal-enriched windows over Denisovan-enriched windows. We selected all windows where %N is greater than 99.999% of all simulations.
- Third, we mirrored the observed distribution of %N around the mean (Supplementary Figure 7.2a,b; dotted density line). This approach identifies windows with a %N greater than the maximum %D.

We identify 11 regions of ~1 Mb as the most extreme outliers of Neandertal ancestry in at least one of these tests (Supplementary Table 7.1).

These regions appear to be homozygous Neandertal, differing from the rest of the genome which is heterozygous Denisovan/Neandertal. For comparison, we next simulated F1 individuals with one *Altai Neandertal*[8] and one *Denisova 3* parent; or one *Altai Neandertal* and one *Vindija 33.19* Neandertal parent; or two *Vindija 33.19* Neandertal parents, sampling DNA fragments using the same conditioning as above. Supplementary Figure 7.3a shows the allele counts for an example

window on chromosome 14. This window falls significantly outside the expected counts for a region with true heterozygous Neandertal/Denisovan ancestry, and is consistent with either *Altai Neandertal-Vindija 33.19* or *Vindija 33.19-Vindija 33.19* regions. For other 1 Mb windows, neither model is a good fit, most likely because they contain a mixture of homozygous Neandertal ancestry and heterozygous Neandertal/Denisovan ancestry (Supplementary Figure 7.3b).

To refine the edges of these windows, we developed a simple three-state Hidden Markov Model (HMM) modelling homozygous Neandertal, homozygous Denisovan, or heterozygous regions, with manually set emission and transition probabilities (see Supplementary Table 7.2). The model uses as input (as emissions) the state of a randomly sampled *Denisova 11* DNA fragment at informative sites (either matching Neandertal or matching Denisovan). For each site, we selected the hidden state with the highest posterior probability, as calculated using the Forward-Backward algorithm implemented in the Python package *pomegranate* (https://github.com/jmschrei/pomegranate).

For 5 regions, the HMM identifies similar ranges of enrichment for Neandertal ancestry as our windowed analysis (Supplementary Figure 7.4a) while for others, the HMM fails to identify a homozygous segment. In these cases, the Neandertal ancestry signal often comes from a small subset of the original 1 Mb window (*e.g.*, chr17:2.4-3.5 Mb, Supplementary Figure 7.4b).

Given the difficulty of identifying smaller homozygous regions without a reasonable recombination map, we conservatively identify 5 regions as homozygous Neandertal, and 6 additional regions as putative homozygous Neandertal. However, we note that additional smaller homozygous Neandertal regions likely exist since an excess of Neandertal-enriched windows compared to both simulations and the mirrored distribution (Supplementary Figure 7.3a,b) is also observed at lower %N thresholds.

Date of older Neandertal admixture

The homozygous Neandertal regions indicate that Neandertal ancestry was present in both parents of *Denisova 11* – that is, the Denisovan father carried Neandertal ancestry. Assuming a constant recombination rate of 1.3×10^{-8} bp^{-1} $generations^{-1}$, the expected length of a block with Neandertal ancestry after N generations is $(N \times 1.3 \times 10^{-8})^{-1}$. An expected length similar to the average length of the regions we detect (0.85 Mb) is observed ~100 generations after admixture, suggesting that the admixture is at least as old as this time.

The total span of the five confidently called regions is 4.2 Mb, showing that at least 0.18% of the callable *Denisova 11* genome (2.762 Gb, requiring at least 50 informative sites in a 1 Mb window) carries homozygous Neandertal ancestry and giving a lower limit for the Neandertal admixture into the Denisovan ancestors of *Denisova 11*. On the other hand, our estimates of Neandertal ancestry (Supplementary Information 4) showed no excess of Neandertal ancestry beyond 50%, suggesting that the proportion of Neandertal ancestry in the Denisovan father is small.

To arrive at a tentative estimate of the number of generations that passed since admixture, we simulated 2.762×10^9 bp genomes undergoing recombination at a constant rate (1.3×10^{-8} bp^{-1} $generations^{-1}$) for varying numbers of generations (between 10 and 1,000) and varying proportions of Neandertal ancestry (between 0.1% and 5%). We then calculated the proportion of 10,000 simulations per combination of parameters in which five regions of homozygous Neandertal ancestry had a length of between 0.72 Mb and 0.95 Mb, and where no longer regions were observed. Supplementary Figure 7.5 shows that simulations had a high probability of generating the observed distribution of the five longest regions when admixture occurred between 300 and 600 generations beforehand. We note that this estimate is tentative at best, since we only model the tail of the distribution and the recombination rate of the regions are assumed to correspond to the genome average. Using two recombination maps[66,67], we find that four regions had a recombination rate below average (0.4-0.9 cM/Mb for [67] and 0.3-0.7 cM/Mb for [66]), while the fifth had an above average recombination rate (1.7 cM/Mb for [67] and 1.6 cM/Mb for [66]), suggesting that the detected regions may be biased towards lower recombination rates. The date of admixture may thus be older than estimated here.

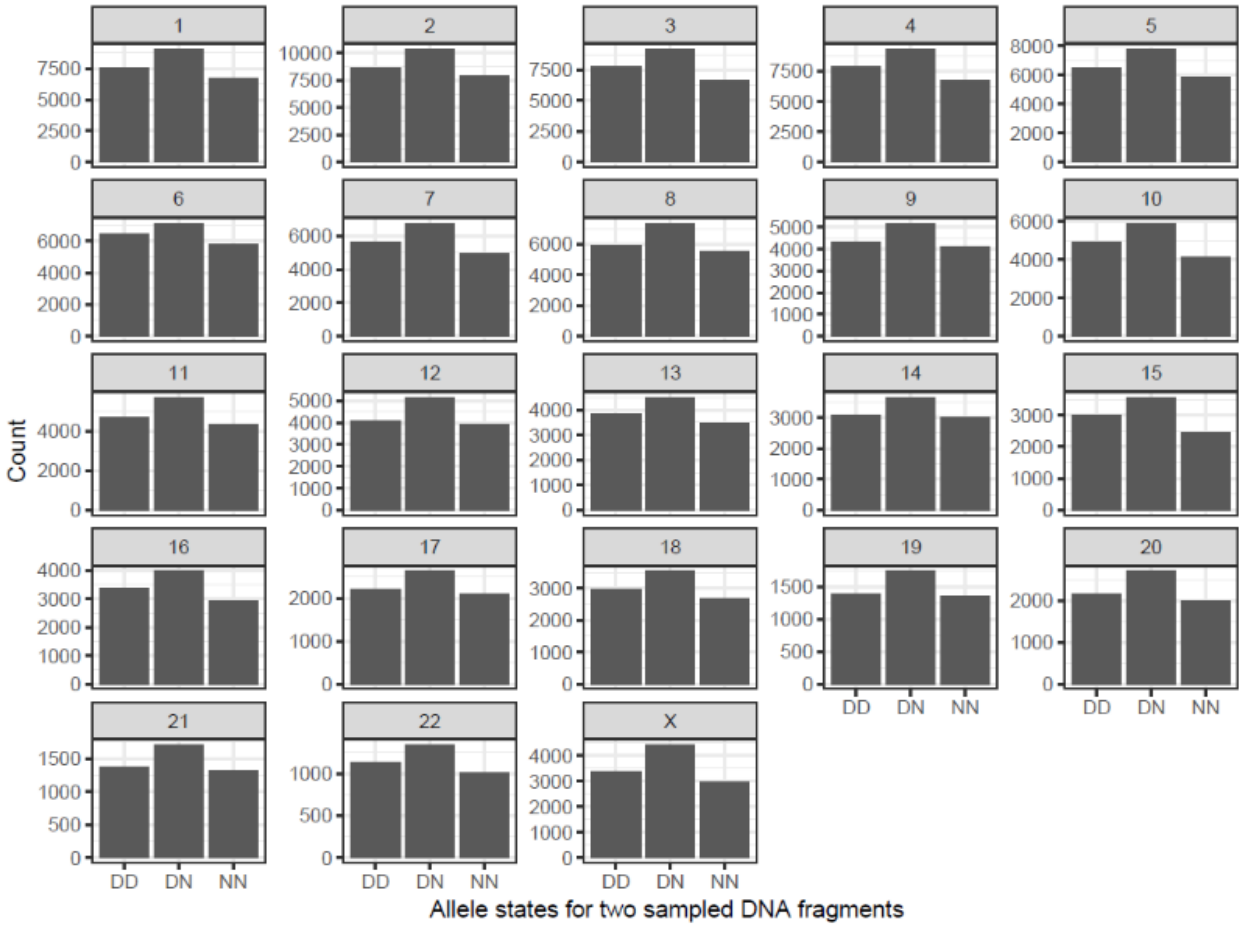

Supplementary Figure 7.1. **Two-allele state counts from *Denisova 11* per chromosome.**

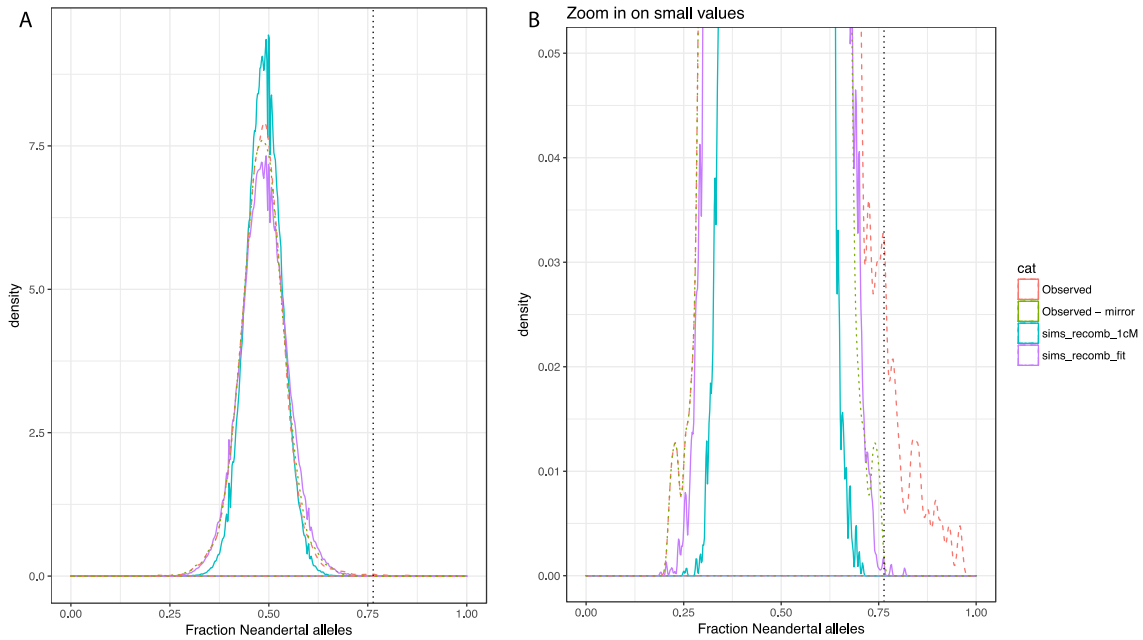

Supplementary Figure 7.2. Distributions of the proportion of Neandertal alleles per 1 Mb window (%N) in *Denisova 11* (red dashed line), simulations with uniform recombination rate 1 Mb = 1 cM (blue line), simulations with fitted uniform recombination rate 1 Mb = 0.3315 cM (purple line), and the *Denisova 11* distribution mirrored around the mean (green dotted line). a. Full distributions. **b.** Y-axis trimmed to highlight the tails of the distributions. Dashed vertical line shows 99.999 quantile of the simulated distribution using a fitted recombination rate. Windows enriched for Neandertal alleles above this line are candidates for homozygous Neandertal regions.

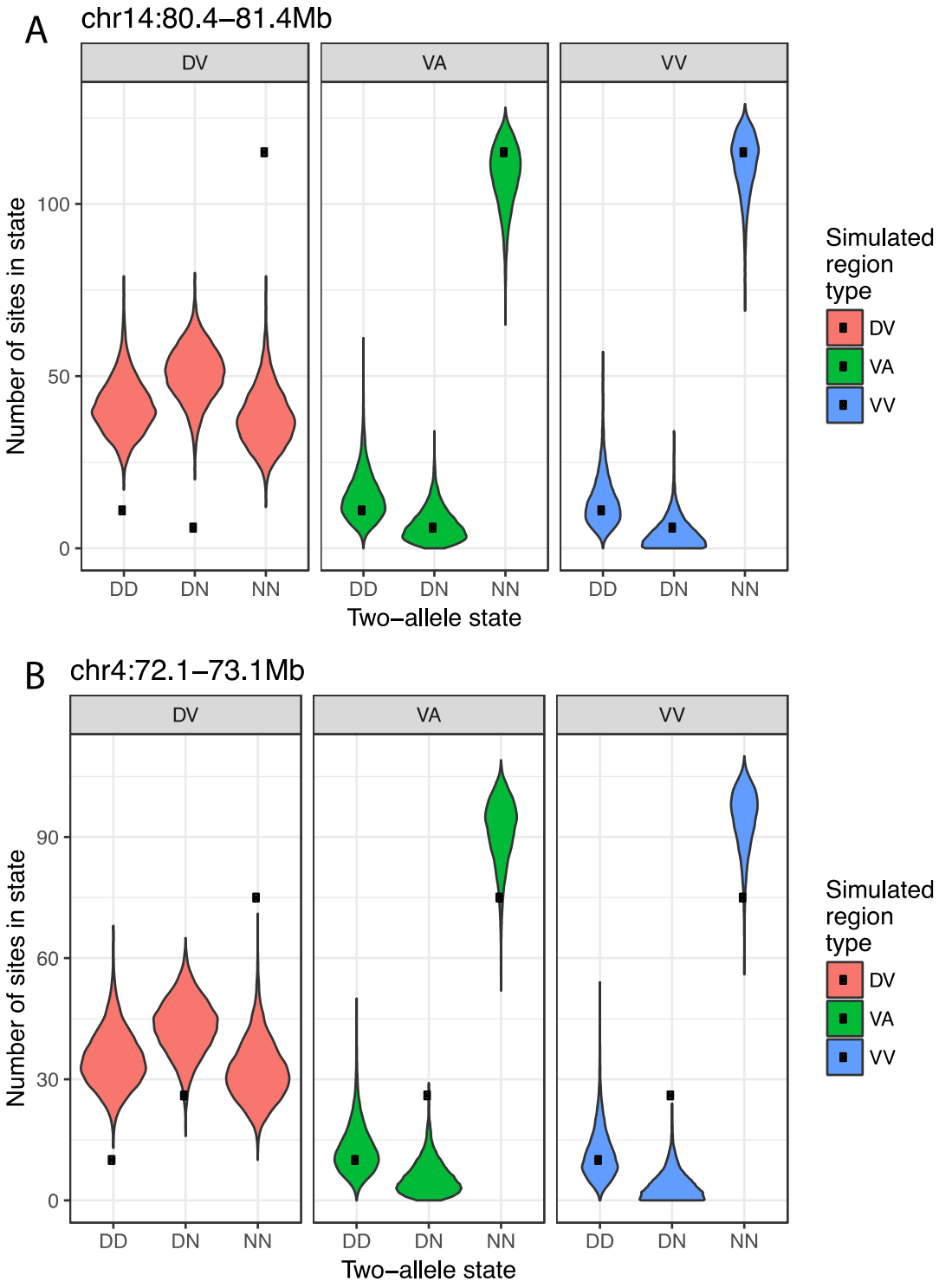

Supplementary Figure 7.3. Two-allele state counts from two example 1 Mb windows enriched for Neandertal sequence (black dots). Violin plots show the distribution of allele counts from simulations (n=10,000 simulations; plots represent raw density of simulated data, with the full range of the data shown) under three models (F1 Denisovan/*Vindija 33.19* (DV), and two homozygous Neandertal models – *Vindija 33.19*/*Altai Neandertal* (VA) and *Vindija 33.19*/*Vindija 33.19* (VV)).

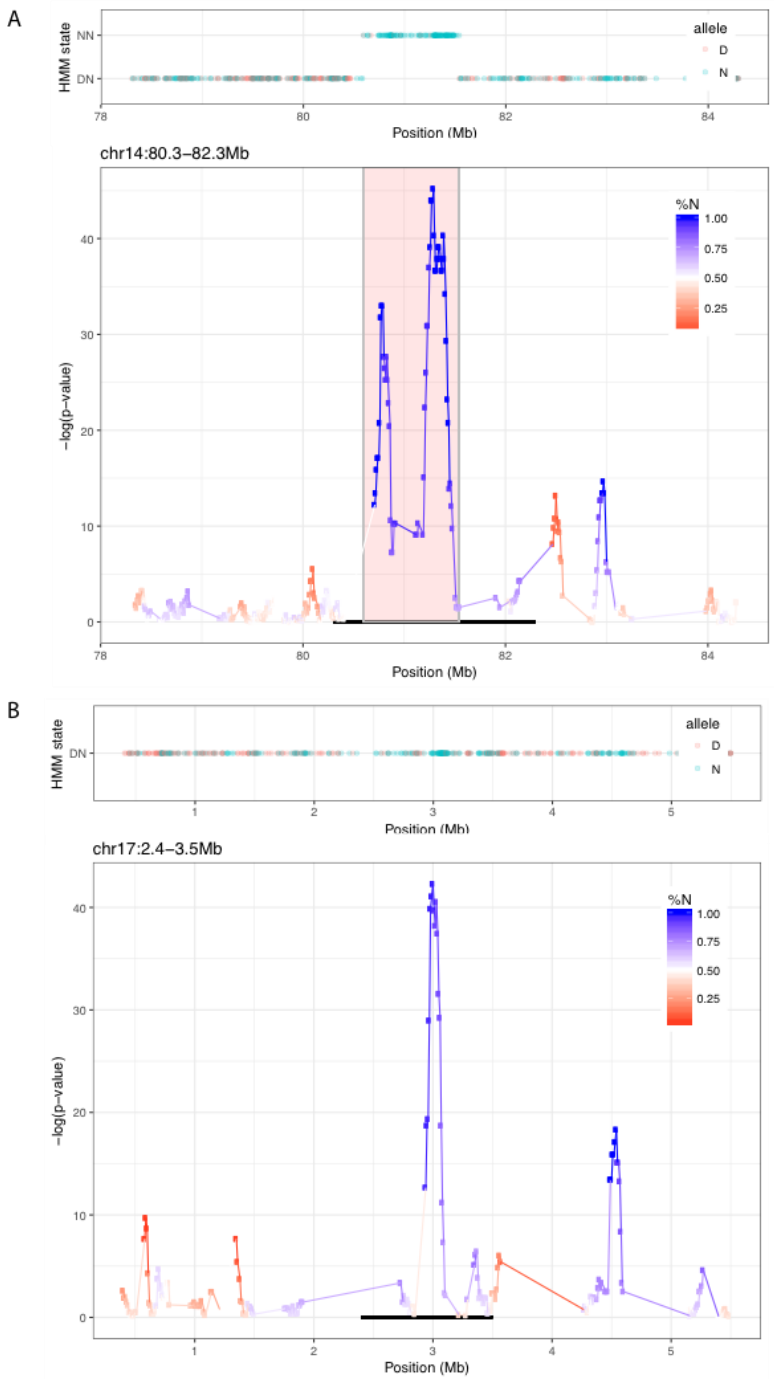

Supplementary Figure 7.4. Example regions enriched for Neandertal ancestry. a. Top panel: all informative alleles, colored by matching a random allele from *Vindija 33.19* (blue) or *Denisova 3* (red). Y-axis is the inferred state: DN heterozygous Denisovan/Neandertal ancestry, NN homozygous Neandertal ancestry. Bottom panel: Chi-square p-values for 100 kb windows (10 kb steps; >10 informative sites required); color shows the proportion of Neandertal alleles. Pink box shows a portion of the region inferred to be homozygous Neandertal via HMM. **b.** Example region enriched for Neandertal ancestry, but with no HMM-called homozygous region.

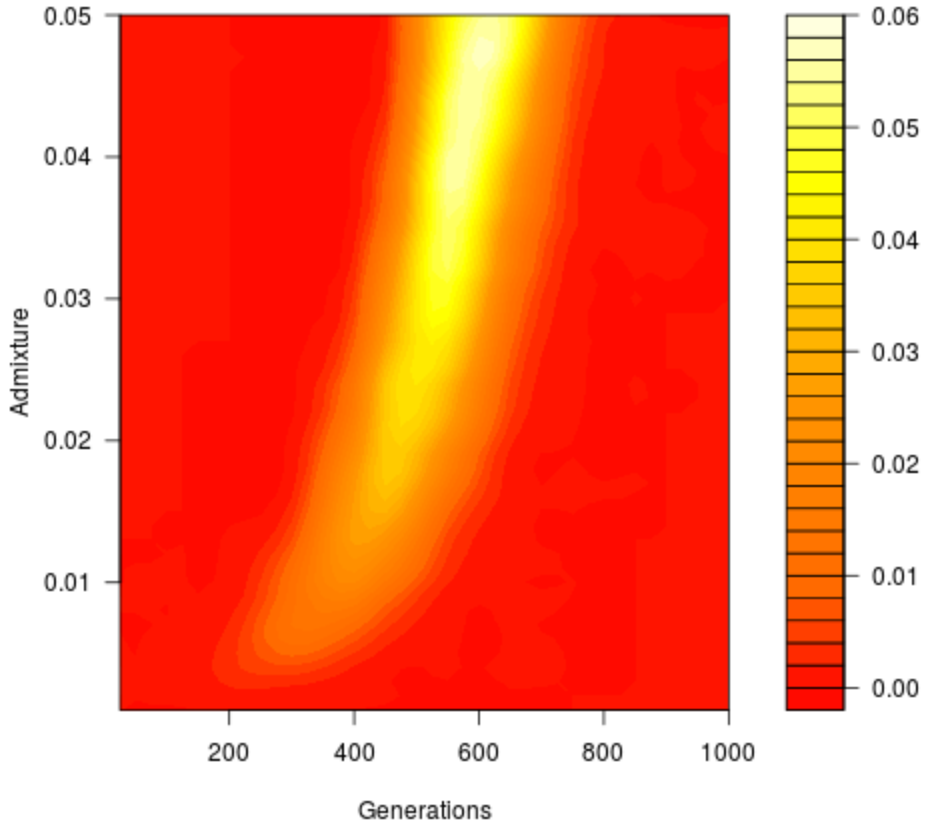

Supplementary Figure 7.5. Proportions of simulations in which the five longest regions of homozygous Neandertal ancestry in *Denisova 11* have length between 0.72 Mb and 0.95 Mb. Lighter colors indicate combinations of number of generations after admixture (Generations, X-axis) and proportion of Neandertal ancestry in *Denisova 11* (Admixture, Y-axis) for which a higher proportion of simulations match the length observed in *Denisova 11*. A total of 10^7 simulations were performed in R (ref. [68]), assuming a constant recombination rate across the genome (1.3×10^{-8} bp^{-1} $generations^{-1}$).

Supplementary Table 7.1. Locations of windows with significant enrichment of Neandertal ancestry. Full regions composed of merged overlapping significant 1 Mb windows. Regions significant by Test 1 (chi-sq) or Test 2 (simulations) are marked with an asterisk (*). All regions are significant by Test 3 (mirrored distribution). If a portion of the window was identified via HMM, that span is given. In other analyses, only the 5 windows identified by the HMM are considered.

Chromosome	Start (Mb)	End (Mb)	Length (Mb)	Chi-sq	Sims	HMM region (Mb)
2	212.8	213.8	1		*	
3	108.4	110.2	1.8	*	*	108.93-109.82
4	71.9	73.4	1.5	*	*	
6	25.2	26.5	1.3	*	*	25.52-26.24
6	31.7	33.5	1.8	*		
6	112	113.7	1.7	*	*	112.63-113.51
9	8.8	10.7	1.9	*	*	9.43-10.18
9	32.8	33.8	1	*	*	
12	28	29.6	1.6	*	*	
14	80.3	82.3	2	*	*	80.59-81.54
17	2.2	3.5	1.3	*	*	

Supplementary Table 7.2. HMM transition and emission probabilities.

		Hidden State		
		NN	**ND**	**DD**
Emission probabilities	Emitting N	.89	.48	.07
	Emitting D	.11	.52	.93
Transition probabilities	State NN	1-1e-9	1e-9	0
	State ND	1e-9	1-2e-9	1e-9
	State DD	0	1e-9	1-1e-9

Supplementary Information 8

The relation of *Denisova 11*'s parents to Neandertal and Denisovan lineages

Summary: To investigate the relatedness of the Neandertal mother of *Denisova 11* to other Neandertals, we compared the proportion of DNA fragments from *Denisova 11* that match derived alleles seen in the two high-coverage Neandertal genomes. At these "informative" positions, *Denisova 11* more often matches the *Vindija 33.19* genome than the *Altai Neandertal*. D-statistics indicate that *Denisova 11* shares more alleles with *Vindija 33.19* and any of the low-coverage Neandertal genomes sequenced to date than with the *Altai Neandertal*. Population split time estimates indicate that the lineage of the Neandertal mother of *Denisova 11* separated from the lineage leading to *Vindija 33.19* ~40,000 years before the latter lived and from the *Altai Neandertal* lineage ~20,000 years before that individual lived; whereas the lineage of the father of *Denisova 11* separated from the lineage leading to *Denisova 3* ~7,000 years before the latter lived.

Allele sharing with other archaic genomes

We evaluated the state of *Denisova 11* fragments at 10,189,394 informative positions, where a randomly sampled allele from at least one previously determined high-coverage genome (*Altai Neandertal*, *Vindija 33.19*, *Denisova 3* or a present-day Mbuti individual)[2,6,8] is derived[1]. Data processing and the determination of the ancestral state were as described in Supplementary Information 4. Whereas 19.6% of *Denisova 11* fragments carry derived alleles matching the *Vindija 33.19* genome, 12.4% carry alleles matching the genome of the *Altai Neandertal* (Supplementary Table 8.1), suggesting a higher affinity of the Neandertal mother of *Denisova 11* with *Vindija 33.19* than with the *Altai Neandertal*.

We used D-statistics[5,13,62] to investigate similarities between the *Denisova 11* genome and previously-sequenced Neandertal and Denisovan genomes. DNA fragments from *Denisova 11* were filtered as described in the Methods section and for base quality higher than 30. A random fragment was sampled at each position from either all fragments sequenced from *Denisova 11*, or from the subset of fragments that showed evidence for deamination in the first three or last three bases. When comparing *Denisova 11* to the high-coverage *Altai Neandertal*, *Vindija 33.19* and *Denisova 3* genomes[2,6,8], s*npAD* genotype calls for the latter genomes at sites that pass the recommended minimal filters (http://cdna.eva.mpg.de/neandertal/Vindija/FilterBed)[2] were used.

For comparisons involving high-coverage and low-coverage data, a random DNA fragment with evidence for deamination was sampled from all genomes. Either the chimpanzee genome[57] (*panTro4*) or the genomes of four Mbuti individuals from the SGDP dataset[28] (filtered for genotype quality ≥ 1) were used as outgroup.

D-statistics[5,13,62] of the form D(A,B,C,O) were calculated across all bi-allelic transversions on the autosomes as

$$D = \frac{\sum(p(BABA) - p(ABBA))}{\sum(p(BABA) + p(ABBA))},$$

with

$$p(ABBA) = (1 - f_A)f_B f_C(1 - f_O) + f_A(1 - f_B)(1 - f_C)f_O,$$
$$p(BABA) = f_A(1 - f_B)f_C(1 - f_O) + (1 - f_A)f_B(1 - f_C)f_O,$$

where f_X denotes the allele frequency in genome/group X at one position (for single genomes: $f_X \in \{0, 0.5, 1\}$ if genotypes are used and $f_X \in \{0, 1\}$ if randomly drawn bases are used).
Standard errors were calculated using a Weighted Block Jackknife[69] over all autosomes divided into 5 Mb blocks.

We first calculated D(Neandertal, *Denisova 3*, *Denisova 11*, chimpanzee) using the high-coverage *Altai Neandertal* and *Vindija 33.19* Neandertal genomes. We used a chimpanzee rather than the Mbuti genomes as outgroup for this comparison because Mbuti individuals share more alleles with Neandertals than with Denisovans[2,8]. D-values range from -1.2% to -5.5% and Z--scores from -2.6 to -16.3 (Supplementary Table 8.2), indicating that *Denisova 11* shares more derived alleles with *Denisova 3* than with either of the two Neandertals, and thus that the Denisovan father of *Denisova 11* was more closely related to *Denisova 3* than the Neandertal mother was to either of the two Neandertals.

Comparing the allele sharing between *Denisova 11* and the two Neandertal genomes, by computing D(*Altai Neandertal*, *Vindija 33.19*, *Denisova 11*, chimpanzee/Mbuti) (Supplementary Table 8.3), yielded D-values of about -22% (|Z| > 17), indicating that the Neandertal mother of *Denisova 11* was more closely related to *Vindija 33.19* from Croatia than to the *Altai Neandertal* from Denisova Cave.

We repeated the analysis using six low-coverage Neandertal genomes from individuals dated to between ~39 kya and ~70 kya *(Goyet Q56-1*, *Les Cottés Z4-1514*, *Mezmaiskaya 1*,

Mezmaiskaya 2, *Spy 94a* and *Vindija 87*)[7,8] (see Figure 1 for their geographical origins, note that *Vindija 87* is the same individual as *Vindija 33.19* (ref. [7])). *Denisova 11* shares more alleles with all these low-coverage Neandertal genomes than it does with the *Altai Neandertal* (Supplementary Table 8.4; D-values between -15% and -23%; $|Z| > 7$), independent of whether the chimpanzee genome or the genomes of four Mbuti individuals were used as outgroup.

When comparing *Denisova 11* to pairs of low-coverage Neandertal genomes, we found that 12 out of 144 comparisons yield a $|Z| > 3$ (Supplementary Table 8.4). However, significant results are obtained only when using the chimpanzee as outgroup, suggesting that these signals are driven by quality differences among samples.

Population split times

The population split times between archaic hominin groups have been determined previously by calculating the statistic F(A|B) between two archaic genomes A and B, where F(A|B) denotes the frequency with which the derived allele at heterozygous sites in B is shared by A[2,8]. This statistic has the advantage of being independent of the demography of population A, since only one random allele is sampled from this population[20]. Thus, we only require knowledge of the demography of population B, which has been estimated for the previously sequenced high-coverage genomes[21]. We computed this statistic using transversions in the two high-coverage Neandertal genomes, *Altai Neandertal* and *Vindija 33.19*, the Denisovan genome (*Denisova 3*), and one Mbuti individual (S_Mbuti-2 from the SGDP dataset[28]). For the calculations, we assume a human-chimpanzee divergence of 13 million years, corresponding to a mutation rate of 0.5×10^{-9} mutation/bp per year[22,29].

The F(A|B) statistics between *Denisova 11* and Mbuti (17.5%; Supplementary Table 8.5) is similar to that observed for other archaic genomes (17.2-17.6%, ref. [2]). The estimated split time of *Denisova 11* from Mbuti is ~530 ky using the population history inferred for the Mbuti by PSMC[2]. Comparing *Denisova 11* to the high-coverage archaic hominin genomes, we find that F(A|B) is highest in the comparison to the *Altai Neandertal* (26.1%), closely followed by *Denisova 3* (25.4%), while the *Vindija 33.19* genome shows the smallest value (21.9%).

However, since *Denisova 11* is an F1 individual, the F(A|B) statistics are expected to yield a 50:50 mixture of the F(A|B) values of the individual's parents:

$$F(\textit{Denisova 11}|B) = F(\text{Neandertal parent of } \textit{Denisova 11}|B)/2 + F(\text{Denisovan parent of } \textit{Denisova 11}|B)/2$$

Thus, F(*Denisova 11*|B) is a composite measure that cannot be directly used to infer the split times of the Neandertal and Denisovan components of *Denisova 11* from the sequenced Neandertal and Denisovan high-coverage genomes, *i.e.,* F(Neandertal parent of *Denisova 11*|Neandertal) and F(Denisovan parent of *Denisova 11*|Denisovan) (Supplementary Figure 8.1).

To obtain these estimates, we take advantage of the fact that the F(A|B) statistic is independent of the specific demographic history of population A, and assume that F(Neandertal parent of *Denisova 11*|Denisovan) = F(Neandertal|Denisovan) for a Neandertal previously sequenced to high-coverage. This is expected since Neandertals appear to be monophyletic with respect to *Denisova 3*, and only minor differences in F(A|B) are observed when different Neandertal genomes are compared to the Denisovan (F(*Vindija 33.19*|*Denisova 3*)=12.3% and F(*Altai Neandertal*|*Denisova 3*)=13.2%, ref. [2]). Similarly, we assume that F(Denisovan parent of *Denisova 11*|Neandertal) = F(Denisovan|Neandertal), *i.e.*, that the lineages leading to different Denisovan genomes separated at a similar time from Neandertals.

We use this assumption to subtract the Denisovan-Neandertal divergence from our F(A|B) values:

$$F(\text{Neandertal parent of } \textit{Denisova 11}|\text{Neandertal}) = 2\,F(\textit{Denisova 11}|\text{Neandertal}) - F(\text{Denisovan}|\text{Neandertal})$$

and

$$F(\text{Denisovan parent of } \textit{Denisova 11}|\text{Denisovan}) = 2\,F(\textit{Denisova 11}|\text{Denisovan}) - F(\text{Neandertal}|\text{Denisovan})$$

The F(A|B) of the Denisovan component of *Denisova 11* and the sequenced Denisovan genome is 37.6% and 37.9%, when using either the *Altai Neandertal* or *Vindija 33.19* as population B to isolate the Denisovan ancestry, respectively (Supplementary Table 8.6). This corresponds to a split time of ~5-10 ky of *Denisova 11* from the *Denisova 3* branch, *i.e.* before the time when *Denisova 3* lived. Since the stratigraphy of Denisova Cave indicates that *Denisova 11* is older than *Denisova 3*, we infer that the Denisovan parent of *Denisova 11* belonged to the ancestral population of *Denisova 3*, or a closely related one. Note that the difference of 0.9% between F(*Vindija 33.19*|*Denisova 3*)=12.3% and F(*Altai Neandertal*|*Denisova 3*)=13.2% does not lead to any noticeable difference in the estimated split times of *Denisova 3* from *Denisova 11* (~6.2 ky versus ~6.8 ky), supporting the assumption that the F(A|B) values of different Neandertals can be used to estimate F(Denisovan parent of *Denisova 11*|Denisovan).

The F(A|B) for the Neandertal component in *Denisova 11* is 35.8% for the *Altai Neandertal* and 31.5% for *Vindija 33.19*. Using the calibration obtained by simulating the demography of the *Altai Neandertal* inferred via PSMC[2], this suggests that the *Altai Neandertal* and *Vindija 33.19* lived ~20 ky and ~40 ky after separating from the Neandertal population that contributed to *Denisova 11*, respectively. These split time estimates, corrected for the sample age inferred by branch-shortening[2], indicate that the Neandertal component of *Denisova 11* separated from the *Altai Neandertal* lineage ~145 kya, and from the lineage leading to *Vindija 33.19* ~100 kya. Previous F(A|B) split time estimates[2] indicate that the *Altai Neandertal* lived ~20 ky after the separation from the lineage leading to *Vindija 33.19*, while *Vindija 33.19* lived ~80 ky after this event. Since the split of *Denisova 11* from *Vindija 33.19* is estimated to be ~40 ky, our results suggest that the Neandertal population leading to *Denisova 11* split off a lineage leading to *Vindija 33.19* about 40 ky after the split from the *Altai Neandertal* (Fig. 4), consistent with that *Denisova 11* shares more alleles with *Vindija 33.19* than with the *Altai Neandertal*.

The results described in Supplementary Information 7 show that the Denisovan parent of *Denisova 11* carried some genomic regions of Neandertal ancestry. To test how these regions influence our estimates of split times of each of the high-coverage archaic genomes from the parents of *Denisova 11*, we repeated the analysis excluding these regions. The inferred split times differ by at most 10.5 ky from the estimates made without removing these regions (*c.f.* Supplementary Tables 8.6 and 8.7). Additionally, we estimated split times assuming that the proportion of Neandertal ancestry in *Denisova 11* is between 48.5% and 51.5%. We estimate that

Denisova 3 lived at most ~10 ky after the split from the lineage leading to the Denisovan parent of *Denisova 11*; while the *Altai Neandertal* and *Vindija 33.19* lived at least ~13 ky and ~28 ky, respectively, after the split from her Neandertal parent (Supplementary Table 8.8). Thus, although the absolute estimates of split times vary when assuming different extents of gene flow, *Denisova 3* is always estimated to have been separated for a shorter time from the Denisovan component of *Denisova 11* than the two Neandertals have been separated from the Neandertal component of *Denisova 11*.

We also carried out simulations to assess to what extent a misspecification of the population size (*Ne*) of Neandertals or Denisovans would influence the split times we infer, by modifying the *Ne* estimates from [2]. When the *Ne* of Denisovans is decreased or increased by 20%, the estimated split times of the Denisovan component of *Denisova 11* from *Denisova 3* change from 6.2-6.8ky (Supplementary Table 8.6) to 5.7-6.5 ky and 6.7-7.5 ky, respectively. When the *Ne* is assumed to be lower or higher by a factor of two, the estimated split times are 3.4-4.3 ky and 11.0-13.2 ky, respectively (Supplementary Table 8.9). When the *Ne* of the *Altai Neandertal* is decreased or increased by 20%, the estimated split times from the Neandertal component of *Denisova 11* are 15.6 ky and 29.3 ky, respectively, and 13.5 ky and 41.6 ky when modified by a factor of two (Supplementary Table 8.9). Thus, although misspecification of the demography may affect the absolute values of the estimated split times, the split times inferred between either of the two high-coverage Neandertal genomes and the Neandertal component of *Denisova 11* are consistently longer than those estimated between *Denisova 3* and the Denisovan component of *Denisova 11*.

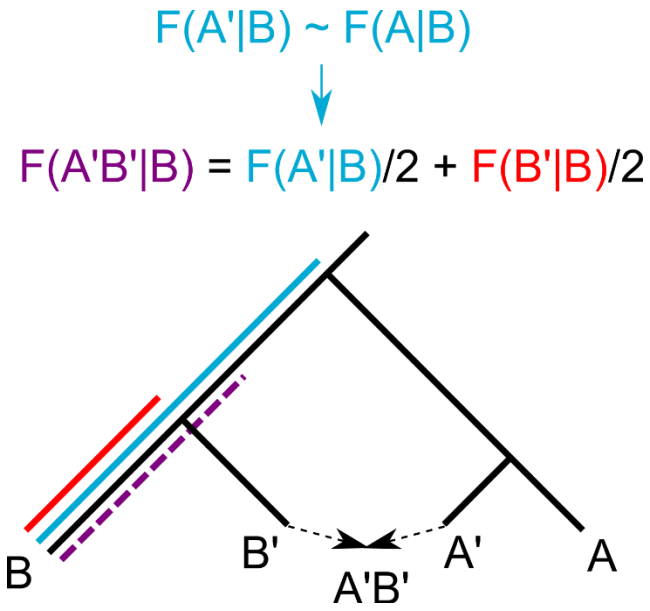

Supplementary Figure 8.1. Scheme for the modified F(A|B). A and B indicate two populations, for example Neandertals and Denisovans. A' and B' refer to the subpopulations from which the parents of *Denisova 11* originate. When the proportion of the two components A' and B' is known, for example 50% in the case of an F1 individual, the F(A|B) statistics computed between the F1 individual and Denisovans (*i.e.*, F(A'B'|B), in purple) can be expressed as a linear combination of the F(A|B) between any Neandertal A and Denisovans B (in blue), and between the Denisovan component of the F1 and the Denisovan genome used as lineage B (in red). Thus, F(A'B'|B) would only provide a split time that is intermediate between that of lineage A' to B, and B' to B (dashed purple line). In order to estimate the split of B' from B, *i.e.*, the split between Denisovans (red line), we subtract the Neandertal component (in blue), that can be estimated using previously known Neandertal genomes[2,8].

Supplementary Table 8.1. Allelic states of *Denisova 11* fragments at "informative" sites. The percentage of fragments matching derived alleles seen in each branch of a tree relating the genomes of two Neandertals (*Altai Neandertal* and *Vindija 33.19*), a Denisovan (*Denisova 3*) and a present-day individual from Africa (Mbuti) are shown, with 95% binomial confidence intervals. Results are shown when using all fragments sequenced from *Denisova 11*, and for fragments carrying putative deamination-induced C to T substitutions at their first three or last three bases. The number of fragments in each analysis is given.

DNA fragments from *Denisova 11*	Number of fragments at informative sites	Matching of derived alleles *(95% CI)*						
					Neandertals			
		All hominins	Shared Neandertal-Denisovan	Shared Neandertal	*Altai Neandertal*	*Vindija 33.19*	Denisovan	Present-day human
All fragments	10,509,928	99.7 *(99.7-99.7)*	97.0 *(97.0-97.1)*	46.8 *(46.7-47.0)*	12.4 *(12.2-12.6)*	19.6 *(19.4-19.8)*	41.3 *(41.2-41.5)*	0.7 *(0.7-0.7)*
Fragments with C to T	2,044,182	99.7 *(99.7-99.8)*	97.1 *(97.0-97.3)*	45.9 *(45.6-46.2)*	11.9 *(11.5-12.2)*	18.6 *(18.2-19.0)*	40.3 *(40.1-40.6)*	0.6 *(0.6-0.7)*

Supplementary Table 8.2. Allele sharing of *Denisova 11* with the *Altai Neandertal, Vindija 33.19* and *Denisova 3*. Results are shown for all fragments generated from *Denisova 11* (Denis11All), and after retaining fragments showing evidence of deamination as attested by a C to T substitution to the reference genome at their first three or last three positions (Denis11Deam). Column #sites refers to the number of ABBA and BABA sites. Rows with |Z|>3 are highlighted.

pop1	pop2	pop3	pop4	D[%]	Z	ABBA	BABA	#sites
Altai Neandertal	*Denisova 3*	Denis11All	chimp	-5.45	-16.32	76292.50	68402.00	159,558
Altai Neandertal	*Denisova 3*	Denis11Deam	chimp	-4.91	-10.02	28107.50	25474.50	59,099
Vindija 33.19	*Denisova 3*	Denis11All	chimp	-1.68	-5.10	75837.00	73325.00	163,152
Vindija 33.19	*Denisova 3*	Denis11Deam	chimp	-1.23	-2.63	27899.50	27221.50	60,304

Supplementary Table 8.3. Comparison of allele sharing with *Denisova 11* between the high-coverage Neandertal genomes. Labelling as in Supplementary Table 8.2.

pop1	pop2	pop3	pop4	D[%]	Z	ABBA	BABA	#sites
Altai Neandertal	*Vindija 33.19*	Denis11All	chimp	-22.99	-24.02	14386.00	9007.50	35,192
Altai Neandertal	*Vindija 33.19*	Denis11All	Mbuti	-22.15	-21.65	14456.66	9213.82	48,304
Altai Neandertal	*Vindija 33.19*	Denis11Deam	chimp	-22.59	-18.51	5305.25	3350.25	12,982
Altai Neandertal	*Vindija 33.19*	Denis11Deam	Mbuti	-22.20	-17.90	5375.84	3422.41	17,989

Supplementary Table 8.4. Allele sharing with *Denisova 11* among six low-coverage and two high-coverage Neandertal genomes. One DNA fragment was drawn randomly from fragments with evidence of deamination from each Neandertal dataset. VindijaUDGDeam, VindijaNonUDGDeam and VindijaAllDeam denote randomly sampled fragments from the UDG-treated, the non-UDG-treated and the pooled libraries of *Vindija 33.19* (ref. [2]), respectively. Other labelling as in Supplementary Table 8.2.

pop1	pop2	pop3	pop4	D[%]	Z	ABBA	BABA	#sites
AltaiDeam	GoyetDeam	Denis11All	chimp	-22.11	-15.25	3134.00	1999.00	5,133
AltaiDeam	GoyetDeam	Denis11All	Mbuti	-19.46	-13.01	2932.00	1976.58	6,642
AltaiDeam	GoyetDeam	Denis11Deam	chimp	-22.88	-10.39	1203.00	755.00	1,958
AltaiDeam	GoyetDeam	Denis11Deam	Mbuti	-20.52	-9.47	1100.58	725.75	2,512
AltaiDeam	LesCottesDeam	Denis11All	chimp	-14.69	-13.09	7917.00	5889.00	13,806
AltaiDeam	LesCottesDeam	Denis11All	Mbuti	-17.88	-14.66	7180.33	5001.83	16,476
AltaiDeam	LesCottesDeam	Denis11Deam	chimp	-16.24	-10.50	2963.00	2135.00	5,098
AltaiDeam	LesCottesDeam	Denis11Deam	Mbuti	-19.22	-11.82	2681.25	1816.63	6,094
AltaiDeam	Mezmais1Deam	Denis11All	chimp	-15.52	-11.22	4037.00	2952.00	6,989
AltaiDeam	Mezmais1Deam	Denis11All	Mbuti	-18.82	-13.11	3663.13	2502.50	8,307
AltaiDeam	Mezmais1Deam	Denis11Deam	chimp	-16.17	-7.70	1476.00	1065.00	2,541
AltaiDeam	Mezmais1Deam	Denis11Deam	Mbuti	-19.17	-9.53	1350.50	915.92	3,060
AltaiDeam	Mezmais2Deam	Denis11All	chimp	-16.98	-13.89	5133.00	3643.00	8,776
AltaiDeam	Mezmais2Deam	Denis11All	Mbuti	-15.27	-11.19	4660.63	3425.92	10,867
AltaiDeam	Mezmais2Deam	Denis11Deam	chimp	-16.78	-9.43	1973.00	1406.00	3,379
AltaiDeam	Mezmais2Deam	Denis11Deam	Mbuti	-15.87	-8.85	1796.38	1304.25	4,215
AltaiDeam	SpyDeam	Denis11All	chimp	-14.53	-8.63	2558.00	1909.00	4,467
AltaiDeam	SpyDeam	Denis11All	Mbuti	-18.37	-10.79	2308.79	1592.21	5,260
AltaiDeam	SpyDeam	Denis11Deam	chimp	-15.27	-6.06	940.00	691.00	1,631
AltaiDeam	SpyDeam	Denis11Deam	Mbuti	-18.04	-7.29	820.33	569.54	1,897
AltaiDeam	Vindija87Deam	Denis11All	chimp	-20.89	-15.82	4560.00	2984.00	7,544
AltaiDeam	Vindija87Deam	Denis11All	Mbuti	-17.77	-12.53	4123.46	2879.21	9,473
AltaiDeam	Vindija87Deam	Denis11Deam	chimp	-20.56	-10.34	1727.00	1138.00	2,865
AltaiDeam	Vindija87Deam	Denis11Deam	Mbuti	-17.99	-9.15	1581.46	1099.29	3,670
AltaiDeam	VindijaAllDeam	Denis11All	chimp	-22.47	-22.70	13200.00	8357.00	21,557
AltaiDeam	VindijaAllDeam	Denis11All	Mbuti	-20.56	-18.97	12128.71	7991.29	27,290
AltaiDeam	VindijaAllDeam	Denis11Deam	chimp	-22.59	-16.62	4884.00	3084.00	7,968
AltaiDeam	VindijaAllDeam	Denis11Deam	Mbuti	-20.30	-14.74	4487.25	2972.96	10,198
AltaiDeam	VindijaNonUDGDeam	Denis11All	chimp	-22.07	-21.93	13193.00	8422.00	21,615
AltaiDeam	VindijaNonUDGDeam	Denis11All	Mbuti	-20.16	-18.06	12094.13	8036.38	27,314
AltaiDeam	VindijaNonUDGDeam	Denis11Deam	chimp	-21.89	-15.98	4892.00	3135.00	8,027
AltaiDeam	VindijaNonUDGDeam	Denis11Deam	Mbuti	-20.42	-14.95	4518.71	2986.13	10,252
AltaiDeam	VindijaUDGDeam	Denis11All	chimp	-22.73	-19.26	7315.00	4605.00	11,920
AltaiDeam	VindijaUDGDeam	Denis11All	Mbuti	-20.28	-16.60	6645.21	4404.54	14,976
AltaiDeam	VindijaUDGDeam	Denis11Deam	chimp	-23.00	-14.05	2717.00	1701.00	4,418
AltaiDeam	VindijaUDGDeam	Denis11Deam	Mbuti	-20.30	-12.40	2475.25	1639.79	5,620
GoyetDeam	LesCottesDeam	Denis11All	chimp	11.20	4.97	1023.00	1281.00	2,304
GoyetDeam	LesCottesDeam	Denis11All	Mbuti	1.14	0.48	967.54	989.79	2,640

GoyetDeam	LesCottesDeam	Denis11Deam	chimp	2.72	0.77	412.00	435.00	847
GoyetDeam	LesCottesDeam	Denis11Deam	Mbuti	-6.01	-1.75	386.17	342.38	990
GoyetDeam	Mezmais1Deam	Denis11All	chimp	6.13	2.22	612.00	692.00	1,304
GoyetDeam	Mezmais1Deam	Denis11All	Mbuti	-2.31	-0.83	584.83	558.46	1,549
GoyetDeam	Mezmais1Deam	Denis11Deam	chimp	7.63	1.61	212.00	247.00	459
GoyetDeam	Mezmais1Deam	Denis11Deam	Mbuti	-4.15	-0.90	206.54	190.08	541
GoyetDeam	Mezmais2Deam	Denis11All	chimp	5.60	2.25	759.00	849.00	1,608
GoyetDeam	Mezmais2Deam	Denis11All	Mbuti	2.80	1.11	706.08	746.79	1,908
GoyetDeam	Mezmais2Deam	Denis11Deam	chimp	3.65	0.95	304.00	327.00	631
GoyetDeam	Mezmais2Deam	Denis11Deam	Mbuti	0.12	0.03	272.21	272.88	738
GoyetDeam	SpyDeam	Denis11All	chimp	12.08	3.19	291.00	371.00	662
GoyetDeam	SpyDeam	Denis11All	Mbuti	2.43	0.62	270.00	283.46	728
GoyetDeam	SpyDeam	Denis11Deam	chimp	9.09	1.44	115.00	138.00	253
GoyetDeam	SpyDeam	Denis11Deam	Mbuti	0.81	0.13	101.88	103.54	273
GoyetDeam	Vindija87Deam	Denis11All	chimp	-0.48	-0.16	632.00	626.00	1,258
GoyetDeam	Vindija87Deam	Denis11All	Mbuti	0.06	0.02	578.08	578.79	1,505
GoyetDeam	Vindija87Deam	Denis11Deam	chimp	-0.22	-0.04	233.00	232.00	465
GoyetDeam	Vindija87Deam	Denis11Deam	Mbuti	0.98	0.22	213.04	217.25	572
LesCottesDeam	Mezmais1Deam	Denis11All	chimp	-0.68	-0.39	1917.00	1891.00	3,808
LesCottesDeam	Mezmais1Deam	Denis11All	Mbuti	-0.06	-0.03	1572.13	1570.21	4,181
LesCottesDeam	Mezmais1Deam	Denis11Deam	chimp	-0.87	-0.32	695.00	683.00	1,378
LesCottesDeam	Mezmais1Deam	Denis11Deam	Mbuti	-2.87	-1.02	599.75	566.33	1,547
LesCottesDeam	Mezmais2Deam	Denis11All	chimp	-6.03	-3.71	2329.00	2064.00	4,393
LesCottesDeam	Mezmais2Deam	Denis11All	Mbuti	0.75	0.44	1859.79	1888.00	5,008
LesCottesDeam	Mezmais2Deam	Denis11Deam	chimp	-6.74	-2.71	903.00	789.00	1,692
LesCottesDeam	Mezmais2Deam	Denis11Deam	Mbuti	-1.11	-0.42	735.75	719.67	1,932
LesCottesDeam	SpyDeam	Denis11All	chimp	-2.95	-1.24	1066.00	1005.00	2,071
LesCottesDeam	SpyDeam	Denis11All	Mbuti	-5.16	-2.05	880.46	794.08	2,215
LesCottesDeam	SpyDeam	Denis11Deam	chimp	0.80	0.22	370.00	376.00	746
LesCottesDeam	SpyDeam	Denis11Deam	Mbuti	-0.12	-0.03	305.33	304.63	790
LesCottesDeam	Vindija87Deam	Denis11All	chimp	-8.08	-4.38	1939.00	1649.00	3,588
LesCottesDeam	Vindija87Deam	Denis11All	Mbuti	0.66	0.35	1500.71	1520.54	4,059
LesCottesDeam	Vindija87Deam	Denis11Deam	chimp	-7.96	-2.93	726.00	619.00	1,345
LesCottesDeam	Vindija87Deam	Denis11Deam	Mbuti	-1.64	-0.58	559.92	541.88	1,511
Mezmais1Deam	Mezmais2Deam	Denis11All	chimp	-1.58	-0.73	1221.00	1183.00	2,404
Mezmais1Deam	Mezmais2Deam	Denis11All	Mbuti	2.50	1.13	1008.25	1059.92	2,739
Mezmais1Deam	Mezmais2Deam	Denis11Deam	chimp	0.11	0.03	446.00	447.00	893
Mezmais1Deam	Mezmais2Deam	Denis11Deam	Mbuti	3.57	1.08	364.38	391.33	1,033
Mezmais1Deam	SpyDeam	Denis11All	chimp	-2.67	-0.90	634.00	601.00	1,235
Mezmais1Deam	SpyDeam	Denis11All	Mbuti	-3.80	-1.27	523.04	484.75	1,338
Mezmais1Deam	SpyDeam	Denis11Deam	chimp	4.87	1.03	215.00	237.00	452
Mezmais1Deam	SpyDeam	Denis11Deam	Mbuti	7.75	1.66	170.71	199.38	489
Mezmais1Deam	Vindija87Deam	Denis11All	chimp	-6.27	-2.81	1051.00	927.00	1,978
Mezmais1Deam	Vindija87Deam	Denis11All	Mbuti	1.62	0.68	847.29	875.25	2,298
Mezmais1Deam	Vindija87Deam	Denis11Deam	chimp	-10.19	-2.78	400.00	326.00	726

Mezmais1Deam	Vindija87Deam	Denis11Deam	Mbuti	1.08	0.31	323.67	330.71	882
Mezmais2Deam	SpyDeam	Denis11All	chimp	3.99	1.45	662.00	717.00	1,379
Mezmais2Deam	SpyDeam	Denis11All	Mbuti	-2.10	-0.75	572.33	548.83	1,513
Mezmais2Deam	SpyDeam	Denis11Deam	chimp	4.59	1.00	239.00	262.00	501
Mezmais2Deam	SpyDeam	Denis11Deam	Mbuti	-0.47	-0.11	205.38	203.46	554
Mezmais2Deam	Vindija87Deam	Denis11All	chimp	-0.87	-0.38	1166.00	1146.00	2,312
Mezmais2Deam	Vindija87Deam	Denis11All	Mbuti	0.46	0.20	1049.58	1059.21	2,798
Mezmais2Deam	Vindija87Deam	Denis11Deam	chimp	0.33	0.10	452.00	455.00	907
Mezmais2Deam	Vindija87Deam	Denis11Deam	Mbuti	2.59	0.79	402.67	424.08	1,100
SpyDeam	Vindija87Deam	Denis11All	chimp	-5.76	-1.89	569.00	507.00	1,076
SpyDeam	Vindija87Deam	Denis11All	Mbuti	1.01	0.32	448.33	457.50	1,209
SpyDeam	Vindija87Deam	Denis11Deam	chimp	-7.73	-1.55	209.00	179.00	388
SpyDeam	Vindija87Deam	Denis11Deam	Mbuti	-1.06	-0.22	165.25	161.79	444
VindijaAllDeam	GoyetDeam	Denis11All	chimp	-1.09	-0.59	1662.00	1626.00	3,288
VindijaAllDeam	GoyetDeam	Denis11All	Mbuti	-0.22	-0.12	1546.54	1539.71	4,074
VindijaAllDeam	GoyetDeam	Denis11Deam	chimp	0.08	0.03	614.00	615.00	1,229
VindijaAllDeam	GoyetDeam	Denis11Deam	Mbuti	-0.22	-0.08	580.29	577.79	1,549
VindijaAllDeam	LesCottesDeam	Denis11All	chimp	7.48	6.10	4673.00	5429.00	10,102
VindijaAllDeam	LesCottesDeam	Denis11All	Mbuti	1.10	0.81	4313.46	4409.54	11,740
VindijaAllDeam	LesCottesDeam	Denis11Deam	chimp	6.54	3.71	1744.00	1988.00	3,732
VindijaAllDeam	LesCottesDeam	Denis11Deam	Mbuti	1.74	0.94	1599.75	1656.46	4,372
VindijaAllDeam	Mezmais1Deam	Denis11All	chimp	5.04	3.35	2697.00	2983.00	5,680
VindijaAllDeam	Mezmais1Deam	Denis11All	Mbuti	-0.78	-0.49	2511.92	2472.83	6,659
VindijaAllDeam	Mezmais1Deam	Denis11Deam	chimp	2.09	0.91	1005.00	1048.00	2,053
VindijaAllDeam	Mezmais1Deam	Denis11Deam	Mbuti	-4.41	-1.93	961.50	880.25	2,475
VindijaAllDeam	Mezmais2Deam	Denis11All	chimp	3.92	2.70	3089.00	3341.00	6,430
VindijaAllDeam	Mezmais2Deam	Denis11All	Mbuti	3.32	2.08	2832.63	3027.00	7,822
VindijaAllDeam	Mezmais2Deam	Denis11Deam	chimp	3.44	1.65	1206.00	1292.00	2,498
VindijaAllDeam	Mezmais2Deam	Denis11Deam	Mbuti	1.98	0.94	1118.42	1163.63	3,050
VindijaAllDeam	SpyDeam	Denis11All	chimp	5.95	3.10	1477.00	1664.00	3,141
VindijaAllDeam	SpyDeam	Denis11All	Mbuti	-0.46	-0.23	1330.29	1318.17	3,530
VindijaAllDeam	SpyDeam	Denis11Deam	chimp	4.65	1.55	544.00	597.00	1,141
VindijaAllDeam	SpyDeam	Denis11Deam	Mbuti	-0.61	-0.20	478.21	472.42	1,249
VindijaAllDeam	Vindija87Deam	Denis11All	chimp	-1.91	-1.03	1332.00	1282.00	2,614
VindijaAllDeam	Vindija87Deam	Denis11All	Mbuti	0.33	0.17	1130.17	1137.63	3,040
VindijaAllDeam	Vindija87Deam	Denis11Deam	chimp	-0.92	-0.29	494.00	485.00	979
VindijaAllDeam	Vindija87Deam	Denis11Deam	Mbuti	1.50	0.49	407.96	420.38	1,129
VindijaAllDeam	VindijaNonUDGDeam	Denis11All	chimp	1.51	1.24	2878.00	2966.00	5,844
VindijaAllDeam	VindijaNonUDGDeam	Denis11All	Mbuti	1.39	1.06	2471.67	2541.25	6,773
VindijaAllDeam	VindijaNonUDGDeam	Denis11Deam	chimp	1.59	0.75	1086.00	1121.00	2,207
VindijaAllDeam	VindijaNonUDGDeam	Denis11Deam	Mbuti	-1.94	-0.91	945.54	909.50	2,525
VindijaAllDeam	VindijaUDGDeam	Denis11All	chimp	-0.18	-0.11	1652.00	1646.00	3,298
VindijaAllDeam	VindijaUDGDeam	Denis11All	Mbuti	-1.74	-0.95	1429.17	1380.29	3,821
VindijaAllDeam	VindijaUDGDeam	Denis11Deam	chimp	-3.59	-1.25	621.00	578.00	1,199
VindijaAllDeam	VindijaUDGDeam	Denis11Deam	Mbuti	-7.35	-2.63	550.71	475.25	1,388

VindijaNonUDGDeam	GoyetDeam	Denis11All	chimp	-2.35	-1.30	1699.00	1621.00	3,320
VindijaNonUDGDeam	GoyetDeam	Denis11All	Mbuti	-1.29	-0.70	1563.17	1523.33	4,069
VindijaNonUDGDeam	GoyetDeam	Denis11Deam	chimp	-3.00	-1.03	635.00	598.00	1,233
VindijaNonUDGDeam	GoyetDeam	Denis11Deam	Mbuti	-0.94	-0.33	568.92	558.29	1,516
VindijaNonUDGDeam	LesCottesDeam	Denis11All	chimp	6.42	5.03	4763.00	5416.00	10,179
VindijaNonUDGDeam	LesCottesDeam	Denis11All	Mbuti	-0.03	-0.02	4382.00	4379.75	11,783
VindijaNonUDGDeam	LesCottesDeam	Denis11Deam	chimp	4.76	2.62	1792.00	1971.00	3,763
VindijaNonUDGDeam	LesCottesDeam	Denis11Deam	Mbuti	1.41	0.75	1599.33	1645.21	4,356
VindijaNonUDGDeam	Mezmais1Deam	Denis11All	chimp	5.28	3.46	2698.00	2999.00	5,697
VindijaNonUDGDeam	Mezmais1Deam	Denis11All	Mbuti	-0.66	-0.42	2530.88	2497.75	6,702
VindijaNonUDGDeam	Mezmais1Deam	Denis11Deam	chimp	1.39	0.62	1027.00	1056.00	2,083
VindijaNonUDGDeam	Mezmais1Deam	Denis11Deam	Mbuti	-4.49	-2.03	973.29	889.63	2,488
VindijaNonUDGDeam	Mezmais2Deam	Denis11All	chimp	3.08	2.13	3098.00	3295.00	6,393
VindijaNonUDGDeam	Mezmais2Deam	Denis11All	Mbuti	2.27	1.42	2829.88	2961.13	7,764
VindijaNonUDGDeam	Mezmais2Deam	Denis11Deam	chimp	2.83	1.36	1220.00	1291.00	2,511
VindijaNonUDGDeam	Mezmais2Deam	Denis11Deam	Mbuti	2.15	1.01	1113.04	1161.96	3,039
VindijaNonUDGDeam	SpyDeam	Denis11All	chimp	5.03	2.57	1473.00	1629.00	3,102
VindijaNonUDGDeam	SpyDeam	Denis11All	Mbuti	-1.54	-0.76	1333.29	1292.83	3,513
VindijaNonUDGDeam	SpyDeam	Denis11Deam	chimp	5.26	1.72	522.00	580.00	1,102
VindijaNonUDGDeam	SpyDeam	Denis11Deam	Mbuti	-0.39	-0.13	472.42	468.71	1,235
VindijaNonUDGDeam	Vindija87Deam	Denis11All	chimp	-2.39	-1.25	1349.00	1286.00	2,635
VindijaNonUDGDeam	Vindija87Deam	Denis11All	Mbuti	-2.17	-1.10	1166.08	1116.50	3,030
VindijaNonUDGDeam	Vindija87Deam	Denis11Deam	chimp	-1.32	-0.41	499.00	486.00	985
VindijaNonUDGDeam	Vindija87Deam	Denis11Deam	Mbuti	0.49	0.15	413.67	417.71	1,105
VindijaNonUDGDeam	VindijaUDGDeam	Denis11All	chimp	-2.81	-1.72	2084.00	1970.00	4,054
VindijaNonUDGDeam	VindijaUDGDeam	Denis11All	Mbuti	-2.64	-1.56	1744.92	1655.25	4,579
VindijaNonUDGDeam	VindijaUDGDeam	Denis11Deam	chimp	-3.75	-1.50	774.00	718.00	1,492
VindijaNonUDGDeam	VindijaUDGDeam	Denis11Deam	Mbuti	-3.14	-1.21	645.58	606.33	1,669
VindijaUDGDeam	GoyetDeam	Denis11All	chimp	-0.97	-0.38	936.00	918.00	1,854
VindijaUDGDeam	GoyetDeam	Denis11All	Mbuti	-1.23	-0.50	872.83	851.63	2,294
VindijaUDGDeam	GoyetDeam	Denis11Deam	chimp	-1.57	-0.41	356.00	345.00	701
VindijaUDGDeam	GoyetDeam	Denis11Deam	Mbuti	-1.04	-0.29	329.17	322.38	877
VindijaUDGDeam	LesCottesDeam	Denis11All	chimp	8.18	5.36	2576.00	3035.00	5,611
VindijaUDGDeam	LesCottesDeam	Denis11All	Mbuti	2.07	1.26	2344.42	2443.71	6,417
VindijaUDGDeam	LesCottesDeam	Denis11Deam	chimp	6.09	2.69	971.00	1097.00	2,068
VindijaUDGDeam	LesCottesDeam	Denis11Deam	Mbuti	2.41	1.02	879.96	923.46	2,402
VindijaUDGDeam	Mezmais1Deam	Denis11All	chimp	4.13	2.07	1473.00	1600.00	3,073
VindijaUDGDeam	Mezmais1Deam	Denis11All	Mbuti	-0.27	-0.13	1367.67	1360.42	3,614
VindijaUDGDeam	Mezmais1Deam	Denis11Deam	chimp	1.43	0.48	551.00	567.00	1,118
VindijaUDGDeam	Mezmais1Deam	Denis11Deam	Mbuti	-1.93	-0.66	524.92	505.08	1,347
VindijaUDGDeam	Mezmais2Deam	Denis11All	chimp	4.36	2.39	1731.00	1889.00	3,620
VindijaUDGDeam	Mezmais2Deam	Denis11All	Mbuti	3.09	1.64	1557.42	1656.83	4,306
VindijaUDGDeam	Mezmais2Deam	Denis11Deam	chimp	6.85	2.46	639.00	733.00	1,372
VindijaUDGDeam	Mezmais2Deam	Denis11Deam	Mbuti	4.36	1.64	606.29	661.63	1,675
VindijaUDGDeam	SpyDeam	Denis11All	chimp	8.56	3.35	796.00	945.00	1,741

VindijaUDGDeam	SpyDeam	Denis11All	Mbuti	2.93	1.16	709.92	752.79	1,914
VindijaUDGDeam	SpyDeam	Denis11Deam	chimp	10.14	2.56	288.00	353.00	641
VindijaUDGDeam	SpyDeam	Denis11Deam	Mbuti	2.26	0.59	264.79	277.04	700
VindijaUDGDeam	Vindija87Deam	Denis11All	chimp	1.26	0.48	707.00	725.00	1,432
VindijaUDGDeam	Vindija87Deam	Denis11All	Mbuti	3.58	1.42	595.29	639.54	1,651
VindijaUDGDeam	Vindija87Deam	Denis11Deam	chimp	5.45	1.25	260.00	290.00	550
VindijaUDGDeam	Vindija87Deam	Denis11Deam	Mbuti	8.49	1.97	207.67	246.21	617

Supplementary Table 8.5. Average F(A|B) values between *Denisova 11* (population A) and high-coverage genomes (population B). Average split times (split from B) are calibrated using the demography of population B, estimated via PSMC. In order to obtain the time of the split in absolute time units (split), we sum the age of genome B estimated via branch shortening (bs) based on transversions (see Table S19 in [2]). Branch shortening and the estimated split times are reported as the percentage of the human-chimpanzee divergence (HC div), as well as in ky and ky before present (kya). Confidence intervals are estimated with a block jackknife with 5 Mb blocks.

popA	popB	F(A|B)	±CI	HC div	split from B (ky)	bs	split (kya)	+ CI (kya)	- CI (kya)
Denisova 11	*Altai Neandertal*	26.1	0.6	1.09	142.1	0.9	264.5	253.5	275.3
	Vindija 33.19	21.9	0.6	1.10	143.2	0.4	194.9	189.7	200.4
	Denisova 3	25.4	0.6	0.68	87.8	0.6	159.8	153.5	167.7
	Mbuti	17.5	0.3	4.07	528.9	0.0	528.9	514.3	544.2

Supplementary Table 8.6. Population split times between archaic genomes and the Neandertal and Denisovan parents of *Denisova 11*. Split times of population B from the Neandertal (N') or Denisovan (D') component of *Denisova 11* are shown. Population A is used to compute F(A|B) as described in the text. Notation as in Supplementary Table 8.5. To illustrate the effect of the uncertainty in age estimates, we used two different branch-shortening estimates to calculate split times before present: branch-shortening based on transversions ("transv" in column sites) and based on all sites ("all" in column sites). Confidence intervals (CIs) are based on block jackknife resampling across the genome (n=523 blocks).

popB	popA	B'	F(B'|B)	±CI	split from B (ky)	bs	sites	split (kya)	+ CI (kya)	- CI (kya)
Denisova 3	*Altai Neandertal*	D'	37.6	0.7	6.8	0.65	all	91.3	89.6	93.0
						0.55	transv	78.8	77.1	80.5
Denisova 3	*Vindija 33.19*	D'	37.9	0.7	6.2	0.65	all	90.7	89.0	92.4
						0.55	transv	78.2	76.5	79.9
Altai Neandertal	*Denisova 3*	N'	35.8	0.7	22.3	0.95	all	145.3	142.9	159.0
						0.94	transv	144.7	142.3	158.5
Vindija 33.19	*Denisova 3*	N'	31.5	0.5	42.2	0.44	all	99.0	87.2	101.6
						0.40	transv	94.0	82.3	96.6

Supplementary Table 8.7. Split times between archaic genomes and the parents of *Denisova 11*, when regions affected by admixture between the two archaic populations are removed. Split times of population B from the Neandertal (N') or Denisovan (D') component of *Denisova 11* are shown. Population A is used to compute F(A|B) as described in the text. Notation as in Supplementary Table 8.6. The 5% top regions that deviate in Neandertal versus Denisovan proportion from the genome-wide average (second test described in Supplementary Information 7) are removed to avoid the influence of previous admixture. Labels for branch-shortening estimates are as in Supplementary Table 8.6. Confidence intervals (CIs) are based on block jackknife resampling across the genome (n=523 blocks).

popB	popA	B'	F(B'|B)	±CI	split from B (ky)	bs	sites	split (kya)	+ CI (kya)	- CI (kya)
Denisova 3	*Altai Neandertal*	D'	36.6	0.8	9.1	0.65	all	93.5	91.8	104.9
						0.55	transv	81.0	79.3	92.4
Denisova 3	*Vindija 33.19*	D'	36.9	0.7	8.5	0.65	all	93.0	91.3	94.7
						0.55	transv	80.5	78.8	82.2
Altai Neandertal	*Denisova 3*	N'	35.6	0.7	32.8	0.95	all	155.8	143.6	160.1
						0.94	transv	155.2	143.0	159.5
Vindija 33.19	*Denisova 3*	N'	30.5	0.5	47.2	0.44	all	103.9	101.3	106.5
						0.40	transv	99.0	96.4	101.6

Supplementary Table 8.8. Population split times between archaic genomes and the Neandertal and Denisovan parents of *Denisova 11* assuming different levels of Neandertal ancestry in *Denisova 11*. Split times of population B from the Neandertal (N') or Denisovan (D') component of *Denisova 11* are shown when different proportions of Neandertal ancestry (%Nea) are assumed to calculate F(B'|B). Population A is used to compute F(A|B) as described in the text. Notation as in Supplementary Table 8.6. Age estimates obtained using branch-shortening based on all sites are shown. Confidence intervals (CIs) are based on block jackknife resampling across the genome (n=523 blocks).

% Nea	popB	popA	B'	F(B'|B)	±CI	split from B (ky)	bs	split (kya)	+ CI (kya)	- CI (kya)
51.5%	*Denisova 3*	*Altai Neandertal*	D'	36.1	0.7	10.2	0.65	94.7	93.0	108.8
	Denisova 3	*Vindija 33.19*	D'	36.4	0.7	9.6	0.65	94.1	92.4	100.3
	Altai Neandertal	*Denisova 3*	N'	37.4	0.7	13.2	0.95	136.2	133.8	142.4
	Vindija 33.19	*Denisova 3*	N'	32.9	0.5	27.9	0.44	84.6	83.3	86.2
50.5%	*Denisova 3*	*Altai Neandertal*	D'	37.1	0.7	7.9	0.65	92.4	90.7	94.1
	Denisova 3	*Vindija 33.19*	D'	37.4	0.7	7.4	0.65	91.8	90.1	93.5
	Altai Neandertal	*Denisova 3*	N'	36.3	0.7	20.6	0.95	143.6	141.2	155.9
	Vindija 33.19	*Denisova 3*	N'	31.9	0.5	30.8	0.44	87.5	85.9	99.5
50.0%	*Denisova 3*	*Altai Neandertal*	D'	37.6	0.7	6.8	0.65	91.3	89.6	93.0
	Denisova 3	*Vindija 33.19*	D'	37.9	0.7	6.2	0.65	90.7	89.0	92.4
	Altai Neandertal	*Denisova 3*	N'	35.8	0.7	22.3	0.95	145.3	142.9	159.0
	Vindija 33.19	*Denisova 3*	N'	31.5	0.5	42.2	0.44	99.0	87.2	101.6
49.5%	*Denisova 3*	*Altai Neandertal*	D'	38.1	0.7	5.7	0.65	90.1	84.5	91.8
	Denisova 3	*Vindija 33.19*	D'	38.4	0.7	5.1	0.65	89.6	84.5	91.3
	Altai Neandertal	*Denisova 3*	N'	35.3	0.7	34.7	0.95	157.7	144.6	161.7
	Vindija 33.19	*Denisova 3*	N'	31.1	0.5	44.3	0.44	101.1	98.4	103.7
48.5%	*Denisova 3*	*Altai Neandertal*	D'	39.2	0.7	0.0	0.65	84.5	84.5	89.6
	Denisova 3	*Vindija 33.19*	D'	39.5	0.7	0.0	0.65	84.5	84.5	84.5
	Altai Neandertal	*Denisova 3*	N'	34.3	0.7	39.9	0.95	162.9	159.3	166.6
	Vindija 33.19	*Denisova 3*	N'	30.2	0.5	48.5	0.44	105.2	102.6	107.8

Supplementary Table 8.9. Population split times between archaic genomes and the Neandertal and Denisovan parents of *Denisova 11*, assuming different demographies for the high-coverage genomes. Split times of population B from the Neandertal (N') or Denisovan (D') component of *Denisova 11* are shown. Population A is used to compute F(A|B) as described in the text. Confidence intervals (CIs) are based on block jackknife resampling across the genome (n=523 blocks). Notation as in Supplementary Table 8.6. The size of population B is decreased or increased by 20% or by a factor of two compared to the PSMC estimates presented in [2]. We varied population sizes by multiplying the theta parameter in the *scrm* code shown in Supplementary Figure 6.1 by 0.5, 0.8, 1, 1.2 or 2.

popB	popA	B'	F(B'|B)	±CI	Split time from B (ky)				
					x0.5	x0.8	x1	x1.2	x2
Denisova 3	*Altai Neandertal*	D'	37.6	0.7	4.3	6.5	6.8	7.5	13.2
Denisova 3	*Vindija 33.19*	D'	37.9	0.7	3.4	5.7	6.2	6.7	11.0
Altai Neandertal	*Denisova 3*	N'	35.8	0.7	13.5	15.6	22.3	29.3	41.6
Vindija 33.19	*Denisova 3*	N'	31.5	0.5	19.7	30.4	42.2	48.1	90.7

Supplementary references

39 Scheuer, L. & Black, S. *Developmental Juvenile Osteology* (Academic Press, San Diego, 2000).

40 Kerley, E. R. The microscopic determination of age in human bone. *Am J Phys Anthropol* **23**, 149-163 (1965).

41 Goldman, H. M., McFarlin, S. C., Cooper, D. M. L., Thomas, C. D. L. & Clement, J. G. Ontogenetic Patterning of Cortical Bone Microstructure and Geometry at the Human Mid-Shaft Femur. *Anat Rec* **292**, 48-64, doi:10.1002/ar.20778 (2009).

42 Streeter, M. A Four-Stage Method of Age at Death Estimation for Use in the Subadult Rib Cortex. *J Forensic Sci* **55**, 1019-1024, doi:10.1111/j.1556-4029.2010.01396.x (2010).

43 Ruff, C. B., Walker, A. & Trinkaus, E. Postcranial Robusticity in Homo .3. Ontogeny. *Am J Phys Anthropol* **93**, 35-54, doi:DOI 10.1002/ajpa.1330930103 (1994).

44 Thompson, J. L. & Nelson, A. J. The place of Neandertals in the evolution of hominid patterns of growth and development. *J Hum Evol* **38**, 475-495, doi:DOI 10.1006/jhev.1999.0364 (2000).

45 Cowgill, L. W. The Ontogeny of Holocene and Late Pleistocene Human Postcranial Strength. *Am J Phys Anthropol* **141**, 16-37, doi:10.1002/ajpa.21107 (2010).

46 Viola, B. *New hominid remains from Central Asia and Siberia: The Easternmost Neanderthals?* (PhD Thesis, University of Vienna, 2009).

47 Trinkaus, E. & Ruff, C. B. Early modern human remains from eastern Asia: The Yamashita-cho 1 immature postcrania. *J Hum Evol* **30**, 299-314, doi:DOI 10.1006/jhev.1996.0025 (1996).

48 Kondo, O. & Dodo, Y. in *Neanderthal burials* (eds Akazawa, T. & Muhesen, S.) 139-214 (KW Publications, Auckland , 2003).

49 Ferembach, D., Schwidetzky, I. & Stloukal, M. Empfehlungen für die Alters- und Geschlechtsdiagnose am Skelett. *Homo: Internationale Zeitschrift Fur Die Vergleichende Forschung Am Menschen* **30**, 1-32 (1979).

50 Viola, B. & Krivoshapkin, A. in *Cultural developments in the Eurasian Paleolithic and the origin of anatomically modern humans* (eds Derevianko, A.P. & Shunkov, M.V.) 172-178 (Publishing Department of the Institute of Archaeology and Ethnography SB RAS, Novosibirsk, 2014).

51 Briggs, A. W. *et al.* Patterns of damage in genomic DNA sequences from a Neandertal. *Proc Natl Acad Sci U S A* **104**, 14616-14621, doi:10.1073/pnas.0704665104 (2007).

52 Krause, J. *et al.* A Complete mtDNA Genome of an Early Modern Human from Kostenki, Russia. *Curr Biol* **20**, 231-236, doi:10.1016/j.cub.2009.11.068 (2010).

53 Prüfer, K. & Meyer, M. Comment on "Late Pleistocene human skeleton and mtDNA link Paleoamericans and modern Native Americans". *Science* **347**, 835, doi:10.1126/science.1260617 (2015).

54 Sawyer, S., Krause, J., Guschanski, K., Savolainen, V. & Pääbo, S. Temporal patterns of nucleotide misincorporations and DNA fragmentation in ancient DNA. *PLoS One* **7**, e34131, doi:10.1371/journal.pone.0034131 (2012).

55 Meyer, M. *et al.* A mitochondrial genome sequence of a hominin from Sima de los Huesos. *Nature* **505**, 403-406, doi:10.1038/nature12788 (2014).

56 The 1000 Genomes Project Consortium. A global reference for human genetic variation. *Nature* **526**, 68-74, doi:10.1038/nature15393 (2015).

57 Mikkelsen, T. S. *et al.* Initial sequence of the chimpanzee genome and comparison with the human genome. *Nature* **437**, 69-87, doi:10.1038/nature04072 (2005).

58 Scally, A. *et al.* Insights into hominid evolution from the gorilla genome sequence. *Nature* **483**, 169-175, doi:10.1038/nature10842 (2012).

59 Locke, D. P. *et al.* Comparative and demographic analysis of orang-utan genomes. *Nature* **469**, 529-533, doi:10.1038/nature09687 (2011).

60 Prüfer, K. *et al.* The bonobo genome compared with the chimpanzee and human genomes. *Nature* **486**, 527-531, doi:10.1038/nature11128 (2012).

61 Green, R. E. *et al.* A complete Neandertal mitochondrial genome sequence determined by high-throughput sequencing. *Cell* **134**, 416-426, doi:10.1016/j.cell.2008.06.021 (2008).

62 Patterson, N. *et al.* Ancient admixture in human history. *Genetics* **192**, 1065-1093, doi:10.1534/genetics.112.145037 (2012).

63 Dabney, J., Meyer, M. & Paabo, S. Ancient DNA Damage. *Csh Perspect Biol* **5**, a012567, doi:10.1101/cshperspect.a012567 (2013).

64 Staab, P. R., Zhu, S., Metzler, D. & Lunter, G. scrm: efficiently simulating long sequences using the approximated coalescent with recombination. *Bioinformatics* **31**, 1680-1682, doi:10.1093/bioinformatics/btu861 (2015).

65 Jensen-Seaman, M. I. *et al.* Comparative recombination rates in the rat, mouse, and human genomes. *Genome Research* **14**, 528-538, doi:10.1101/gr.1970304 (2004).

66 Kong, A. *et al.* Fine-scale recombination rate differences between sexes, populations and individuals. *Nature* **467**, 1099-1103, doi:10.1038/nature09525 (2010).

67 Hinch, A. G. *et al.* The landscape of recombination in African Americans. *Nature* **476**, 170-175, doi:10.1038/nature10336 (2011).

68 R Core Team. *R: A language and environment for statistical computing*. (R Foundation for Statistical Computing, 2016).

69 Busing, F. M. T. A., Meijer, E. & Van Der Leeden, R. Delete-m jackknife for unequal m. *Stat Comput* **9**, 3-8, doi:Doi 10.1023/A:1008800423698 (1999).